

**NASA TECHNICAL NOTE**



**NASA TN D-2118**

*C.1*

LOAN COPY: RET  
AFWL (WLL  
KIRTLAND AFB.



NASA TN D-2118

# **EFFECT OF SEEDING AND ION SLIP ON ELECTRON HEATING IN A MAGNETOHYDRODYNAMIC GENERATOR**

*by Frederic A. Lyman, Arthur W. Goldstein,  
and John E. Heighway*

*Lewis Research Center  
Cleveland, Ohio*



0154609

EFFECT OF SEEDING AND ION SLIP ON ELECTRON HEATING  
IN A MAGNETOHYDRODYNAMIC GENERATOR

By Frederic A. Lyman, Arthur W. Goldstein,  
and John E. Heighway

Lewis Research Center  
Cleveland, Ohio

NATIONAL AERONAUTICS AND SPACE ADMINISTRATION

For sale by the Office of Technical Services, Department of Commerce,  
Washington, D.C. 20230 -- Price \$1.25

## EFFECT OF SEEDING AND ION SLIP ON ELECTRON

### HEATING IN A MAGNETOHYDRODYNAMIC

### GENERATOR<sup>1</sup>

#### SUMMARY

The influence of electron-ion collisions on the attainment of high electron temperatures and their corresponding effects on conductivity and power density in magnetohydrodynamic generators have been examined theoretically. For argon seeded with various small amounts of cesium, it was found that the presence of seed is actually deleterious to electron heating. The maximum electron temperature, conductivity, and power density are attained without seed. The effect of ion slip has also been analyzed, and the value of the ratio of magnetic field to gas pressure for maximum power density has been determined for unseeded argon.

#### INTRODUCTION

The magnetohydrodynamic (MHD) power generator, which converts the kinetic energy of a conducting fluid directly into electrical energy, has shown promise of becoming an important energy-conversion device (ref. 1). One of the fundamental problems with this device has been the attainment of a sufficiently high equilibrium electrical conductivity of the gas at the static temperatures that are attained in practical generators.

Since the useful electrical power produced by the generator is proportional to the kinetic energy of the gas flowing through it, high gas velocities are desirable. To provide such high velocities, a large portion of the initial thermal energy of the gas must be converted into kinetic energy, and this process reduces the static gas temperature and, therefore, the equilibrium degree of ionization and conductivity. One means of providing a sufficiently high conductivity at the static gas temperature involves preheating the gas and seeding it with an alkali vapor (e.g., cesium or potassium) of low ionization potential. In several experimental devices (refs. 2 to 4), combustion gases have been used, which required a flow-through cycle. At the attainable gas temperatures (2000° to 3000° K), only the seed vapor becomes ionized to any appreciable extent.

---

<sup>1</sup>A brief summary of some of the results presented in this report was given at the Fourth Symposium on Engineering Aspects of Magnetohydrodynamics, Berkeley, California, April 10-11, 1963.

The apparent limitation imposed by the maximum permissible gas temperature may, in fact, be circumvented by nonequilibrium ionization processes. The process of electron heating has attracted considerable attention as a means of providing an adequate degree of ionization even at comparatively low gas temperatures. In this process, the electrons gain energy from the induced electric fields. On elastic collision with ions or atoms, the directed energy of the electrons is converted into random or thermal energy. The electrons lose energy in these collisions, but, because of the large disparity in mass between the electron and its collision partner, this energy loss is a very small fraction of the initial kinetic energy of the electron (ref. 5, p. 474). Consequently, in a strong electric field the electrons may acquire a mean thermal energy that greatly exceeds the mean thermal energy of the gas. Moreover, because of their high energies, the electrons may cause further ionization on collision with the gas atoms.

The presence of electron heating in gas-discharge phenomena was recognized by early workers in the field of gaseous electronics (ref. 6). More recently, Kerrebrock (ref. 7) noted that the measured conductivity of a potassium-seeded argon plasma was larger than that which could be provided by equilibrium ionization at the gas temperature. Kerrebrock assumed that this effect was due to electron heating and proposed a simple theory to predict the conductivity at elevated electron temperatures. The essential feature of this theory is that the ionization and volume recombination processes are assumed to be in equilibrium at the electron temperature. The Saha equation, which is based on equilibrium thermodynamics and statistical mechanics (e.g., see derivations in ref. 5, p. 427 and ref. 8), is used to calculate the degree of ionization, but the electron temperature is used in place of the equilibrium gas temperature. Kerrebrock found that the predicted variation of conductivity with both current density and gas temperature was in agreement with the experimental results and therefore concluded that the assumption of ionization equilibrium at the electron temperature was justified. The validity of the application of the equilibrium Saha equation to the nonequilibrium case of ionization at elevated electron temperatures has been established for a cesium plasma by Ben Daniel and Tamor (ref. 9). The results show that the Saha equation is an excellent approximation for electron temperatures in excess of 0.3 electron volt and cesium gas densities greater than  $10^{14}$  atoms per cubic centimeter.

The application of Kerrebrock's theory to various configurations of MHD generators was carried out by Hurwitz, Sutton, and Tamor (ref. 10). In that paper, as in Kerrebrock's analysis, the electron temperature was determined by equating the rate of energy gain by the electrons from the induced electric fields to the rate of energy loss in elastic collisions with the neutral gas atoms. Because of the low degrees of ionization attained, electron-ion collisions were assumed to occur infrequently and their contribution to the energy transfer was negligible. A somewhat similar analysis of the performance of MHD generators with electron heating was made independently by Wright and Swift-Hook (ref. 11), and electron-ion collisions were also neglected by them.

The neglect of electron-ion collisions is not justified, even for low degrees of ionization. If a monatomic gas with a small cross section is used, calculation shows that the electron temperature may become so high that a degree

of ionization is attained at which electron-ion collisions are the dominant momentum and energy interchange process. Because of the large coulomb cross section for electron-ion collisions, such a situation may occur at a quite minute degree of ionization. Dougal and Goldstein (ref. 12) have shown experimentally that, under certain conditions in gas discharges, the energy exchange between the electrons and ions predominates even when the degree of ionization is less than 0.001 percent.

The object of the present report is to assess the effect of electron-ion collisions on the attainment of high electron temperatures and the performance of MHD generators. This effect is studied with particular reference to the optimum conditions of operation of the generator, particularly the optimum degree of seeding and the optimum gas pressure.

### MOMENTUM AND ENERGY EQUATIONS

A partially ionized, electrically neutral mixture of monatomic gases is considered. The gas mixture consists of atoms (A) and singly charged ions ( $A^+$ ) of the carrier gas, atoms (S) and singly charged ions ( $S^+$ ) of the seed gas, and electrons (e). (Symbols are defined in appendix A.) The gas moves as a whole with velocity  $\vec{u}$  perpendicular to a uniform static magnetic field of intensity  $\vec{B}$ . As a result of this motion an induced electric field  $\vec{u} \times \vec{B}$  is set up, which together with the electric field  $\vec{E}$ , pressure gradients, and other forces causes the various species of particles to move with drift velocities  $\vec{w}_r$  ( $r = A, A^+, S, S^+$ ) relative to the mean gas flow. Furthermore, the charged particles may absorb energy from the electric field and acquire temperatures that exceed the mean static temperature  $T$  of the gas mixture.

In principle, it is possible to determine the temperatures and velocities of the various species by considering a system of five momentum and five energy equations, one for each species, in conjunction with other equations describing other properties that may be involved. Since all these equations are coupled, such a general program clearly involves a prohibitive degree of complexity. A much simpler system of equations will be used herein. These equations are considerably simplified versions of momentum and energy transfer equations that were derived by Burgers in references 13 and 14 from the Boltzmann equation. The simplifications are described in appendix B and are equivalent to the neglect of spatial nonuniformities in the properties of the electrons and ions, but some attempt is made in appendix B to justify the neglect of such terms. Of perhaps more significance than the neglect of nonuniformities is the fact that the basic equations derived in references 13 and 14 neglect inelastic collisions. Inelastic collisions will also be neglected herein.

The simplified momentum equations are

$$e_r(\vec{E}^* + \vec{w}_r \times \vec{B}) = \sum_t \frac{m_r m_t}{m_r + m_t} \nu_{rt} (\vec{w}_r - \vec{w}_t) \quad (1)$$

( $r = e, A^+, S^+; t = e, A^+, S^+, A, S$ )

Equation (1) simply expresses a balance between the rate of increase in the average momentum of species  $r$  due to the action of the Lorentz force (left side) and the rate of momentum loss through collisions with all other species (right side). Here,  $e_r$  and  $m_r$  are, respectively, the charge and the mass of a particle of species  $r$ , and  $\vec{E}^*$  is the effective electric field in a system of coordinates moving with the mean gas velocity  $\vec{u}$ ; that is,

$$\vec{E}^* = \vec{E} + \vec{u} \times \vec{B} \quad (2)$$

where  $\vec{E}$  is the electric field (v/m) in the laboratory coordinate system, and  $\vec{B}$  is the intensity of the magnetic field (webers/sq m). As mentioned before,  $\vec{w}_r$  is the mean drift velocity of species  $r$ , that is, the velocity relative to the gas velocity  $\vec{u}$ . The mean collision frequency for momentum transfer from species  $r$  to species  $t$  is denoted by  $\nu_{rt}$ . The expressions for the various quantities  $\nu_{rt}$  will be presented in the section Collision Frequencies.

It should be pointed out that the momentum equations are written only for the electrons and the ions. The further assumption is made here that the drift velocities of both the seed and the carrier gases are negligible. Since the atoms are not subject to the electric forces that give rise to the drift velocities of the charged species, this is certainly a reasonable assumption.

The temperatures of all atom and ion species are assumed to be equal to the static temperature  $T$  of the gas mixture, excluding the electrons (see appendix B). Therefore, the only energy equation that will be considered is the following simplified energy equation for the electrons:

$$-e w_e \cdot \vec{E}^* = \frac{3}{2} k(T_e - T) \sum_{t \neq e} \frac{2m_e}{m_t} \nu_{et} \quad (3)$$

where  $e$  is the magnitude of the charge of an electron, and  $k$  is the Boltzmann constant. Equation (3) balances the rate of gain of energy by the electrons from the effective electric field  $\vec{E}^*$  with the rate of loss of energy in elastic collisions with atoms and ions.

Although inelastic collisions are not considered here, in some cases they may be taken into account by using an appropriately modified collision frequency. In references 7 and 10, a mean loss factor is introduced on the right side of equation (3) in the term referring to electron-neutral collisions. This factor accounts for the energy lost by the electrons in exciting the vibrational and rotational energy levels of a molecule on collision. Since this factor may be large, a polyatomic gas is generally disadvantageous for electron heating. Thus, attention is restricted here to monatomic gases.

Equations (1) and (3), together with the Saha equations, which predict the degrees of ionization of the carrier gas and seed as a function of electron temperature, form the basis of the subsequent analysis. The Saha equations are presented in the next section. Then the problem is treated in two parts. In the

first part it is assumed that ion slip is negligible. This means that the density of the neutral gas is sufficiently high and the fields sufficiently low that collisions between the atoms and the ions effectively constrain the ions to move at the gas velocity; that is, the drift velocities of the ion species may be taken to be zero. For the case of negligible ion slip, the seeded gas will be treated, and particular attention will be paid to the question of the optimum degree of seeding.

Ion slip may become important for strong magnetic fields or low gas densities. Thus, the effect of ion slip is considered in the second part of the problem. For this case it is sufficient to consider an unseeded gas, for reasons that will appear later.

#### DEGREE OF IONIZATION OF A SEEDED GAS

The degree of ionization of a seeded gas is obtained on the basis of Kerrebrock's assumption (ref. 7), that the volume ionization and recombination processes are in equilibrium at the electron temperature and that the Saha equation is valid. In previous analyses (refs. 7 and 10), it has been assumed that only the seed provides an appreciable number of ions and electrons; however, in anticipation of high electron temperatures, the ionization of both the seed and the carrier gas will be considered here. Thus, it is necessary to solve the following two Saha equations (ref. 15):

For  $S \rightleftharpoons S^+ + e$ :

$$\frac{N_e N_{S^+}}{N_S} = \frac{2g_{S^+}}{g_S} \left( \frac{2\pi m_e kT_e}{h^2} \right)^{3/2} \exp \left[ - \frac{eV_S}{kT_e} \right] \quad (4)$$

For  $A \rightleftharpoons A^+ + e$ :

$$\frac{N_e N_{A^+}}{N_A} = \frac{2g_{A^+}}{g_A} \left( \frac{2\pi m_e kT_e}{h^2} \right)^{3/2} \exp \left[ - \frac{eV_A}{kT_e} \right] \quad (5)$$

In these equations,  $V_S$  and  $V_A$  are the first ionization potentials of the seed and the carrier gas, respectively,  $h$  is the Planck constant, and  $g_{S^+}$ ,  $g_S$ ,  $g_{A^+}$ , and  $g_A$  are the ground-state degeneracies of the respective ions and atoms. A table of these degeneracies for several gases is given in reference 16.

Before ionization takes place, let there be  $N_A^0$  atoms of the carrier gas and  $N_S^0$  atoms of the seed per unit volume. Then

$$\left. \begin{aligned} N_A^0 &= N_A + N_{A^+} \\ N_S^0 &= N_S + N_{S^+} \end{aligned} \right\} \quad (6)$$

The equations (4) to (6) together with the condition of charge neutrality

$$N_e = N_{A^+} + N_{S^+} \quad (7)$$

are sufficient for the determination of  $N_e$  as a function of  $T_e$  once  $N_A^0$  and  $N_S^0$  have been specified.

Numerical solution of these equations is required, and an iteration method is convenient. Since the ionization potential of the carrier gas is usually several times that of the seed, this method may be carried out as follows. For the first approximation,  $N_{A^+}$  may be set equal to zero in equation (7) and  $N_{S^+}$  calculated from equation (4). This value of  $N_{S^+}$  is then used with equations (5) and (7) to calculate  $N_{A^+}$ . The process is repeated with the value obtained for  $N_{A^+}$ . This procedure was found to converge quite rapidly.

## GENERATOR WITH SEEDED GAS

### Current-Temperature-Field Relations

To determine the electron temperature from the electron energy equation (3), it is first necessary to obtain the electron drift velocity from equation (1). Here it is assumed that  $\vec{w}_r = 0$  for  $r = A, A^+, S, S^+$ ; hence, all the momentum equations (1) except that for the electrons may be discarded.

If the electron mass is neglected when it appears in the sum  $m_e + m_t$  ( $t \neq e$ ) and the total collision frequency  $\nu_e$  is introduced, the electron momentum equation may be written as

$$-e(\vec{E}^* + \vec{w}_e \times \vec{B}) = m_e \nu_e \vec{w}_e \quad (8)$$

where

$$\nu_e = \sum_{t \neq e} \nu_{et} \quad (9)$$

It is convenient to formulate the problem in terms of the electron current density

$$\vec{J}_e = -N_e e \vec{w}_e \quad (10)$$

which in the case of no ion slip is also the total current. Equation (8) may be written as

$$\vec{J}_e - \beta_e \frac{\vec{B}}{B} \times \vec{J}_e = \sigma_0 \vec{E}^* \quad (11)$$

where  $\sigma_0$  is the scalar conductivity

$$\sigma_0 = \frac{N_e e^2}{m_e v_e} \quad (12)$$

and  $\beta_e$  is the electron Hall parameter, which is defined as

$$\beta_e = \frac{\omega_e}{v_e} = \frac{eB}{m_e v_e} \quad (13)$$

where  $\omega_e = eB/m_e$  is the electron cyclotron frequency.

It will be assumed that there is no component of the electrostatic field  $\vec{E}$  in the direction of the magnetic field; hence, the effective field  $\vec{E}^*$  and the current are perpendicular to  $\vec{B}$ . This assumption is based on the fact that the two walls of the generator duct that are perpendicular to the magnetic field are insulators with no potential difference between them. Equation (11) may be easily solved for  $\vec{J}_e$  by multiplying both sides by the vector operator  $(1 + \beta_e \frac{\vec{B}}{B} \times)$  and by noting that, because  $\vec{B} \cdot \vec{J}_e = 0$ ,

$$\frac{\vec{B}}{B} \times \left( \frac{\vec{B}}{B} \times \vec{J}_e \right) = -\vec{J}_e$$

The result is

$$\vec{J}_e = \frac{\sigma_0}{1 + \beta_e} (\vec{E}^* + \beta_e \frac{\vec{B}}{B} \times \vec{E}^*) \quad (14)$$

The second term in the parentheses on the right side of equation (14) represents the Hall field, which is perpendicular to both  $\vec{B}$  and  $\vec{E}^*$ .

The energy equation (3) is rewritten as

$$\vec{J}_e \cdot \vec{E}^* = \frac{3}{2} k(T_e - T) \nu_E N_e \quad (15)$$

where  $\nu_E$  is the effective collision frequency for energy transfer defined as

$$\nu_E = \sum_{t \neq e} \frac{2m_e}{m_t} \nu_{et} \quad (16)$$

The energy equation (15) may be recast in the following manner: Either  $\vec{J}_e$  may be eliminated by means of equation (14), so that a relation is obtained be-

tween the electron temperature  $T_e$  and the effective field  $\vec{E}^*$ , or  $\vec{E}^*$  may be eliminated by means of equation (11), so that an equation relating  $J_e$  and  $T_e$  is obtained. The latter choice is adopted here. From equation (11), it follows that

$$\vec{J}_e \cdot \vec{E}^* = \frac{J_e^2}{\sigma_0} \quad (17)$$

hence, equation (15) may be written as

$$J_e^2 = 3 \frac{e^2 k}{m} \delta (T_e - T) N_e^2 \quad (18)$$

where  $m$  is the mass of an atom of the carrier gas and  $\delta$  is defined as

$$\delta = \frac{1}{2} \frac{m}{m_e} \frac{\nu_E}{\nu_e} = \frac{\sum_{t \neq e} \frac{m}{m_t} \nu_{et}}{\sum_{t \neq e} \nu_{et}} \quad (19)$$

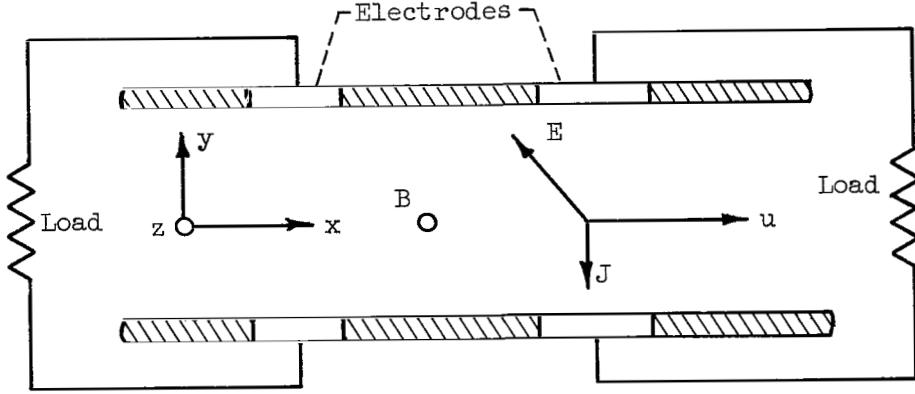
It can be seen from equation (19) that  $\delta$  is of the order of  $m/m_t$ , where the subscript  $t$  corresponds to the atom or the ion species with the largest collision frequency  $\nu_{et}$ . For argon seeded with cesium,  $\delta$  may vary between  $m_{Ar}/m_{Cs} \approx 0.3$  and 1. For an unseeded gas,  $\delta \approx 1$ . Thus, in the cases of interest in this report,  $\delta$  is only weakly dependent on the magnitude of the collision frequencies, so that equation (18) is virtually independent of the collision frequencies.

#### Solution for Segmented Generator

For purposes of calculation, it is convenient to proceed in the following manner: An electron temperature is assumed, and the electron number density calculated from equations (4), (5), and (7). The magnitude of the current is then determined by means of equation (18), once the collision frequencies have been found and  $\delta$  has been calculated. The corresponding effective field  $\vec{E}^*$  is obtained from equation (11) to determine the generator operating point. Since only the magnitude of the current can be found from equation (18), it is necessary to have a condition on the direction of either the current or the electric field. This condition is obtained from consideration of the generator configuration.

The configuration of a segmented electrode generator to be considered is shown in the following sketch. This configuration has been proposed to eliminate the axial Hall current and thus improve the generator performance (refs. 1 and 10). Each pair of electrodes is connected to a separate load, and the loads are adjusted so that there is an axial electric field  $E_x$ , which just balances

the Hall field  $\beta_e E_y^*$ . Thus, no current flows in the x-direction.



For simplicity, it is assumed that the electrodes are so finely segmented that their structure introduces no nonuniformities into the flow. If  $J_{e,x}$  is set equal to zero in equation (11), the current is

$$J_{e,y} = \sigma_o E_y^* = \sigma_o (E_y - uB) \quad (20)$$

It is customary to define a load parameter  $K$  as the ratio of the voltage across the electrodes to the open circuit voltage, that is

$$K \equiv \frac{E_y}{uB} = 1 + \frac{J_{e,y}}{\sigma_o uB} = 1 + \frac{E_y^*}{uB} \quad (21)$$

For open circuit  $K = 1$ , whereas for short circuit  $K = 0$ , and the short-circuit current is  $J_{e,y} = -\sigma_o uB$ . The maximum rate of electron heating occurs with a short circuit, since

$$\vec{J}_e \cdot \vec{E}^* = \sigma_o E_y^{*2} = \sigma_o u^2 B^2 (1 - K)^2 \quad (22)$$

After the magnitude of the current has been obtained from equation (18), the load parameter is calculated from the relation

$$K = 1 - \frac{J_e}{\sigma_o uB} \quad (23)$$

where

$$J_e = |J_{e,y}|$$

It should be noted that, although equation (18) is virtually independent of the collision frequency, equation (23) indicates that the relation between the current and the electric field involves the collision frequency through the conductivity  $\sigma_o$ .

The power density (power developed per unit volume) is

$$P = -\vec{J}_e \cdot \vec{E} \quad (24)$$

For the segmented generator, the power density is

$$P = \sigma_0 u^2 B^2 K(1 - K) \quad (25)$$

The calculation of current, conductivity, load parameter, and power density for a specified electron temperature may be carried out in a straightforward manner from the preceding equations. The value of  $T_e$  for which  $K$  becomes zero is the maximum electron temperature; electron temperatures between this value and the gas temperature  $T$  correspond to load parameters between 0 and 1. To carry out these calculations, the collision frequencies must be known.

### Collision Frequencies

In Burgers' notation (ref. 13), the average collision frequency  $\nu_{rt}$  for momentum transfer from species  $r$  to species  $t$  is

$$\nu_{rt} = \frac{2}{3} N_t \alpha Z_{rt}^{(11)} \quad (26)$$

where  $Z_{rt}^{(11)}$  is the cross section for momentum transfer averaged over all scattering angles and relative velocities of the colliding particles and  $\alpha$  is a mean thermal speed:<sup>2</sup>

$$\alpha^2 = \frac{2kT_r}{m_r} + \frac{2kT_t}{m_t} \quad (27)$$

In the case of collisions between electrons and ions or atoms, clearly,  $\alpha$  may be approximated by the mean electron thermal speed  $\sqrt{2kT_e/m_e}$ .

For collisions between electrons and atoms, the hard elastic sphere model gives (see eqs. 130a and 131, ref. 13)

---

<sup>2</sup>In most of the development of reference 13, the temperatures  $T_r$  and  $T_t$  are assumed to be nearly equal to the mean gas temperature  $T$ , so that  $\alpha^2 = 2kT/\mu$ , where  $\mu = m_r m_t / (m_r + m_t)$ . This assumption is removed in Section 25 of that reference, however, and it is shown there that for the energy equation the only change is that  $\alpha^2$  is replaced by equation (27) (see first equation at the top of p. 118, ref. 13). By an extension of Burgers' analysis to the case of arbitrary temperature differences between species ( $T_r - T_t$ ), it is possible to show that the same modification of  $\alpha^2$  is also the only essential change in the momentum transfer equation. (The method outlined in reference 17 may be utilized in proving the preceding statement.).

$$Z_{ea}^{(11)} = \frac{4}{\sqrt{\pi}} (\pi \sigma^2) \quad (28)$$

where  $\sigma$  is a distance of the order of the radius of the atom. In this report, however, the experimentally determined value of the cross section for electron-atom collisions  $Q_{ea}$  will be used in place of  $\pi \sigma^2$ . The electron-atom collision frequency is then written as

$$\nu_{ea} = \frac{4}{3} N_a Q_{ea} \left( \frac{8kT_e}{\pi m_e} \right)^{1/2} \quad (a = A, S) \quad (29)$$

For collisions between electrons and ions, the cross section is (see eq. 147, ref. 13, rewritten here in mks units)

$$Z_{ei}^{(11)} = 2 \sqrt{\pi} \left( \frac{e^2}{4\pi\epsilon_0 kT_e} \right)^2 \ln \Lambda \quad (30)$$

where from equation 150, reference 13

$$\Lambda = \frac{12\pi(\epsilon_0 kT_e)^{3/2}}{e N_i^{1/2}} = 1.24 \times 10^7 \frac{T_e^{3/2}}{N_i^{1/2}} \quad (\text{mks units}) \quad (31)$$

The electron-ion collision frequency is then

$$\nu_{ei} = \frac{e^4}{6(2m_e)^{1/2} \epsilon_0^2 (\pi k)^{3/2}} \frac{N_i \ln \Lambda}{T_e^{3/2}} = 3.63 \times 10^{-6} \frac{N_i \ln \Lambda}{T_e^{3/2}} \quad (\text{mks units}) \quad (32)$$

Before the results for generator performance are presented, it is of interest to compare the various collision frequencies for a seeded gas over a range of electron temperatures. Such a comparison will aid in the interpretation of the subsequent results.

A cesium-seeded argon plasma is considered. The following conditions, which are appropriate to an MHD generator, are assumed: an argon number density  $N_A^0 = 1.1 \times 10^{18}$  per cubic centimeter and a cesium number density  $N_S^0 = 1.1 \times 10^{16}$  per cubic centimeter, or 1-percent cesium seed. (This argon density corresponds to a generator operating at Mach 3, a stagnation temperature of 2500° K, and a stagnation pressure of 3 atm.) For argon, the atom and the ion degeneracies are, respectively,  $g_{Ar} = 1$  and  $g_{Ar+} = 6$ , while for cesium,  $g_{Cs} = 2$  and  $g_{Cs+} = 1$  (ref. 16). The ionization potentials of argon and cesium are 15.68 and 3.89 volts, respectively.

The degrees of ionization  $N_{A+}/N_A^0$  and  $N_{S+}/N_S^0$  of argon and cesium are calculated for various electron temperatures from the Saha equations (4) and (5), and the results are shown in figure 1. It can be seen that the 1-percent cesium seed becomes nearly fully ionized at an electron temperature slightly above  $5000^\circ \text{K}$ . The degree of ionization of argon is insignificant below electron temperatures of  $7000^\circ \text{K}$ . When the electron temperature reaches  $10,000^\circ \text{K}$ , however, the number densities of argon and cesium ions are comparable.

Experimental values for the electron-atom cross sections are required to calculate the collision frequencies. The average cross section for argon was taken to be  $2.0 \times 10^{-17}$  square centimeter, which is approximately the value at the Ramsauer minimum (ref. 18).

There is some disparity in the data available for electron-cesium cross sections at electron energies less than 1 electron volt. The mean momentum transfer cross section reported in reference 19 decreases from  $10.6 \times 10^{-14}$  square centimeter at an electron temperature of  $450^\circ \text{K}$  to  $8.5 \times 10^{-14}$  square centimeter at  $550^\circ \text{K}$ . Unfortunately, this temperature range is too narrow to cover the cases of interest here in which the electron temperature may be considerably higher. On page 311, reference 20, a constant cesium cross section of  $1.3 \times 10^{-14}$  square centimeter is quoted as an applicable value for electron energies in the range 0.1 to 0.5 electron volt ( $1160^\circ$  to  $5800^\circ \text{K}$ ). According to the older data of reference 21, which do not go below about 0.5 electron volt, the cesium cross section is approximately  $3.3 \times 10^{-14}$  square centimeter at this energy. In reference 22, cross sections were reported in the range 0.05 to 0.062 electron volt, values considerably lower than those cited previously (about  $1/20$  of values of ref. 19). Finally, theoretical elastic cross sections for cesium were derived in reference 23. The theoretical momentum transfer cross section decreases from  $4 \times 10^{-14}$  square centimeter at an electron temperature of  $1000^\circ \text{K}$  to  $2 \times 10^{-14}$  square centimeter at  $10,000^\circ \text{K}$ .

In view of the disparity of these data, for the purposes of the calculations in this report, a constant value of  $3.3 \times 10^{-14}$  square centimeter was taken for the electron-cesium collision cross section. This value agrees with the data of reference 21 and the theoretical values of reference 23. It may also be noted that the extrapolation of the data of reference 19 toward 1 electron volt approaches the value given in reference 21 (see fig. 3, ref. 19).

The collision frequencies for the electrons with the various constituents of a cesium-seeded argon plasma are shown as a function of the electron temperature in figure 2. The same conditions as for figure 1 are assumed. For clarity, the collision frequencies with the two ion species were calculated separately. From figure 2 it is clear that, at electron temperatures above  $2500^\circ \text{K}$ , the electron-ion collision frequency is the dominant one. Also, because of the presence of seed, the total collision frequency  $\nu_e$  behaves in an unusual manner, first increasing rapidly until the seed is nearly fully ionized (at about  $5000^\circ \text{K}$ ), then decreasing slowly until, at about  $9000^\circ \text{K}$ , the ionization of argon causes it to rise again.

## Performance of Segmented Generator

For the segmented generator, electron temperature, conductivity, power density, and Hall parameter were calculated as a function of the load parameter for argon seeded with various small amounts of cesium. The static gas temperature  $T$  and static pressure  $p$  were referred to the stagnation temperature  $T_0$  and pressure  $p_0$  by the usual relations for isentropic expansion, which are good approximations for small degrees of ionization:

$$\frac{p_0}{p} = \left(1 + \frac{\gamma - 1}{2} M^2\right)^{\frac{\gamma}{\gamma - 1}} \quad (33)$$

$$\frac{T_0}{T} = 1 + \frac{\gamma - 1}{2} M^2 \quad (34)$$

where  $M$  is the Mach number of the flow near the entrance of the generator. The gas velocity is

$$u = M \sqrt{\gamma \frac{k}{m} T} \quad (35)$$

For a monatomic gas such as argon, the ratio of specific heats is  $\gamma = 5/3$ .

The following conditions were chosen for the calculations for which the results are shown in figures 3 to 5: stagnation pressure,  $p_0$ , 3 atmospheres; stagnation temperature,  $T_0$ , 2500° K; Mach number  $M$ , 3. For these conditions the initial number density of the argon in the generator  $N_A^0$  is  $1.1 \times 10^{18}$  per cubic centimeter, as in figures 1 and 2. The gas velocity is 1400 meters per second, and the gas temperature is 625° K.

Calculations were carried out for two magnetic-field strengths, 0.2 and 2 webers per square meter (2000 and 20,000 gauss, respectively) and several values of the seed fraction. The stronger field was chosen to be of the same order as the fields achieved in present experimental generators (refs. 1 to 4). It might be expected that, with a relatively weak magnetic field, the effective electric field  $E^*$  would be reduced to such an extent that electron heating would be insignificant. To establish whether this was, in fact, the case, the weaker field of 0.2 weber per square meter was also picked.

For these two magnetic-field strengths and the aforementioned gas conditions, the load parameter was calculated as a function of the electron temperature from equations (20) and (25). The electron temperature is plotted against the load parameter in figure 3. It may be noted that, for the segmented generator, the highest electron temperature is attained with a short circuit. The most striking facts about figure 3 are that for both magnetic-field strengths the electron heating is appreciable and that the highest electron temperature for any value of the load parameter is attained for an unseeded plasma. It is also interesting to note that, to certain values of the load parameter, there

correspond two or three electron temperatures. Depending on how the field is varied, some of these points may represent unstable states. The unusual shape of the curves for seeded argon arises from the behavior of the total collision frequency  $\nu_e$  with increasing electron temperature illustrated by the solid curve in figure 2.

The reduction of the magnetic field from 2 to 0.2 weber per square meter produces a comparatively small percentage reduction in electron temperature. For unseeded argon, the electron temperature decreases by 20 to 30 percent when the magnetic field is reduced. With the addition of seed, however, the electron temperature is depressed even more in the case of the weaker magnetic field. For example, for  $B = 2$  webers per square meter and 1 percent seed, the electron temperature may still reach  $9000^\circ \text{K}$  for sufficiently small load parameters, but with  $B = 0.2$  weber per square meter, the presence of 1 percent seed depresses the electron temperature to values below  $3000^\circ \text{K}$  for all load parameters.

The electron temperature is, by itself, an inadequate indication of generator performance. Therefore, the conductivity and power density are plotted against load parameter in figures 4 and 5, respectively. The curves of figure 4 for conductivity are quite similar to the curves of figure 3, as might be expected, since, when electron-ion collisions dominate, the conductivity varies as  $T_e^{3/2}$ . For both magnetic-field strengths and for all values of the load parameter, the conductivity is the greatest for the unseeded gas.

The curves of figure 5 for power density show the effect of seeding on generator performance most clearly. It can be seen that, for all values of the load parameter, the highest power density is achieved without seeding. As the percentage of seed is increased, the sharp reduction in power density extends to lower values of the load parameter. The reduction of the magnetic field from 2 to 0.2 weber per square meter is accompanied by a drop in the power density of more than two orders of magnitude. The factor  $B^2$  in the expression (25) for the power density is responsible for most of this drop, the remainder being caused by a smaller conductivity due to the lower electron temperature. Furthermore, for the weaker magnetic field, the same percentage of seed causes a larger percentage reduction in the power density, as can be seen by comparing the curves of figures 5(a) and (b) for 0.1 and 1 percent seed.

The fact that seed actually impairs performance may be explained as follows. Although the seed ionizes much more easily than the gas at relatively low temperatures (less than  $5000^\circ \text{K}$ ), the total electron collision frequency also increases because of collisions with the ions provided by the seed. The electron temperature is reduced somewhat by the energy lost in these collisions. The conductivity, which when electron-ion collisions dominate is virtually independent of the electron number density and varies as  $T_e^{3/2}$ , is then also reduced. Thus, whenever the electron temperature attains a level at which electron-ion collisions dominate (which may occur at relatively low temperatures, of the order of  $2500^\circ \text{K}$ ), the addition of seed results in a drop in performance.

Since electron-ion collisions limit the attainable electron temperature in all cases considered here, the results will not be sensitive to the disparities in the cesium atom cross section mentioned previously. A significant change in

the calculated results would appear only if the actual cesium cross section turns out to be larger than the value used here by more than an order of magnitude. Even if that were the case, the conclusion that seeding inhibits electron heating would still be substantiated.

Finally, it is interesting to compare the values of the Hall parameter  $\beta_e$  for the two magnetic fields, 0.2 and 2 webers per square meter. The Hall parameter is plotted against the load parameter in figure 6. Comparison of figures 6(a) and (b) shows that, except in the neighborhood of  $K = 1$ , the Hall parameter is increased only slightly when the magnetic field is increased by a factor of 10. This is a consequence of the fact that the collision frequency  $\nu_e$  is nearly the same as the electron-ion frequency  $\nu_{ei}$ , which is proportional to  $N_e$  and inversely proportional to  $T_e^{3/2}$ . The stronger magnetic field results in higher electron temperatures and consequently more ionization, and calculations show that  $\nu_e$  increases in roughly the same proportion as  $B$ . The fact that  $\beta_e$  is almost independent of  $B$  when electron heating is appreciable means that comparisons of generator performance should not be based on  $\beta_e$ , as was done in references 10 and 11.

#### EFFECT OF ION SLIP IN ABSENCE OF SEED

Since the power density is roughly proportional to  $B^2$ , clearly, it is desirable to use the strongest possible magnetic field. Furthermore, it is expected that electron heating would be enhanced by decreasing the density of the gas, since the collision frequency would thereby be reduced. It has been suggested (ref. 24), however, that ion slip would present a definite limitation on the gain that could be realized from these attempts.

In this section, the effect of ion slip will be considered. Because of the results of the previous section, seed will not be used, and a three-component mixture consisting of electrons and ions and atoms of the carrier gas will be analyzed.

#### Current-Temperature-Field Relations

Momentum equations of the form of equation (1) are written for the electrons and ions. Again the drift velocity of the gas atoms is neglected. When  $m_e$  is neglected in the sum  $m_e + m_t$  ( $t = i, a$ ), the momentum equations become

$$m_e \nu_{ei} (\vec{w}_e - \vec{w}_i) + m_e \nu_{ea} \vec{w}_e = -e(\vec{E}^* + \vec{w}_e \times \vec{B}) \quad (36)$$

$$m_e \nu_{ie} (\vec{w}_i - \vec{w}_e) + \frac{m}{2} \nu_{ia} \vec{w}_i = e(\vec{E}^* + \vec{w}_i \times \vec{B}) \quad (37)$$

where  $m$  is the mass of a gas atom.

The electron current is

$$\vec{J}_e = -N_e e \vec{w}_e \quad (38)$$

while the total current is

$$\vec{J} = N_e e (\vec{w}_i - \vec{w}_e) \quad (39)$$

Since  $N_e = N_i$ , the collision frequencies  $\nu_{ie}$  and  $\nu_{ei}$  are equal. Equations (36) and (37) may be written as follows in terms of the currents  $\vec{J}_e$  and  $\vec{J}$ :

$$-m_e \nu_{ei} \vec{J} - m_e \nu_{ea} \vec{J}_e = -N_e e^2 \vec{E}^* + e \vec{J}_e \times \vec{B} \quad (40)$$

$$m_e \nu_{ei} \vec{J} + \frac{m}{2} \nu_{ia} (\vec{J} - \vec{J}_e) = N_e e^2 \vec{E}^* + e (\vec{J} - \vec{J}_e) \times \vec{B} \quad (41)$$

Equations (40) and (41) are added to eliminate  $\vec{E}^*$ , and the resulting equation may be rearranged to give the following relation between  $\vec{J}_e$  and  $\vec{J}$ :

$$\vec{J}_e = \frac{1}{1 + \epsilon} \left( \vec{J} + \beta_i \frac{\vec{B}}{B} \times \vec{J} \right) \quad (42)$$

where  $\beta_i$  is the ion Hall parameter defined as

$$\beta_i = 2 \frac{\omega_i}{\nu_{ia}} = 2 \frac{eB}{m \nu_{ia}} \quad (43)$$

and

$$\epsilon = 2 \frac{m_e}{m} \frac{\nu_{ea}}{\nu_{ia}} \quad (44)$$

Equation (42) is substituted back into equation (41), and the resulting equation may be written as follows for the component of  $\vec{J}$  perpendicular to  $\vec{B}$ :

$$\sigma_0 \vec{E}^* = \frac{1}{1 + \epsilon} \left[ \left( 1 + \beta_e \beta_i + \frac{\epsilon \nu_{ei}}{\nu_e} \right) \vec{J} - (1 - \epsilon) \beta_e \frac{\vec{B}}{B} \times \vec{J} \right] \quad (45)$$

where  $\sigma_0$  is the conductivity as defined in equation (12).

From equations (26) to (28) the ion-atom collision frequency may be written

$$\nu_{ia} = \frac{4}{3} \frac{\sqrt{2}}{N_a Q_{ia}} \left( \frac{8kT}{\pi m} \right)^{1/2} \quad (46)$$

and thus,

$$\epsilon = \sqrt{2} \frac{Q_{ea}}{Q_{ia}} \left( \frac{m_e}{m} \frac{T_e}{T} \right)^{1/2} \quad (47)$$

Since the ratio  $Q_{ea}/Q_{ia}$  is ordinarily less than 1 and since  $T_e/T$  is of order 10 for the cases of interest here,  $\epsilon$  is much less than 1. Hence, it will be neglected in comparison to 1 in equations (42) and (45), which become

$$\vec{J}_e = \vec{J} + \beta_i \frac{\vec{B}}{B} \times \vec{J} \quad (48)$$

$$\sigma_o \vec{E}^* = (1 + \beta_e \beta_i) \vec{J} - \beta_e \frac{\vec{B}}{B} \times \vec{J} \quad (49)$$

Equation (49) may be solved for the component of  $\vec{J}$  perpendicular to  $\vec{B}$  to yield

$$\vec{J} = \frac{\sigma_o}{(1 + \beta_e \beta_i)^2 + \beta_e^2} \left[ (1 + \beta_e \beta_i) \vec{E}^* + \beta_e \frac{\vec{B}}{B} \times \vec{E}^* \right] \quad (50)$$

which, except for the factor 2 in the definition of  $\beta_i$ , is identical with equation (27) of reference 10.<sup>3</sup>

Equations (48) and (49) may be used to write the rate of electron heating  $\vec{J}_e \cdot \vec{E}^*$  in terms of the total current as the rather simple expression

$$\vec{J}_e \cdot \vec{E}^* = \frac{J^2}{\sigma_o} \quad (51)$$

Thus, the energy equation in the form of equation (18) may be applied to the ion-slip problem also simply by writing  $J$  for  $J_e$ . The main changes will appear in the expression for the load parameter in terms of the current.

#### Solution for Segmented Generator

For the segmented electrode generator, the assumption is again made that the field  $E_x$  suppresses the Hall current, so that  $J_x = 0$ . In place of equation (23), the following expression is obtained by setting  $J_x = 0$  in equation (49):

$$K = 1 - (1 + \beta_e \beta_i) \frac{J}{\sigma_o u B} \quad (52)$$

where the definition of the load parameter  $K$  is unchanged, and  $J = |J_y|$ .

The same program of calculation that was used before can be employed. The electron temperature is specified,  $J$  is calculated from equation (18), and  $K$

<sup>3</sup>This difference evidently arises because  $m$  was used in reference 10 for the reduced mass, rather than the correct value  $m/2$ .

is determined from equation (52). Note that, for the same electron temperature (and consequently the same current), the value of  $K$  calculated from equation (52) is smaller than that calculated from equation (23) with ion slip neglected. In other words, with ion slip, a larger field is required to attain the same electron temperature, so that ion slip reduces electron heating.

The power density for the segmented generator is

$$P = -J_y E_y = \frac{\sigma_0}{1 + \beta_e \beta_i} K(1 - K) u^2 B^2 \quad (53)$$

Thus, ion slip reduces the power density in two ways. First, because of the lower electron temperature,  $\sigma_0$  is reduced, and a second reduction is made by the factor  $(1 + \beta_e \beta_i)^{-1}$ .

In equations (52) and (53), ion slip enters through the product of the Hall parameters  $\beta_e \beta_i$ . To calculate  $\beta_i$ , the ion-atom collision frequency is required. In the calculations of this report, the collision frequency is obtained from experimental data on ion mobility. The ion mobility is defined as (ref. 25, p. 61)

$$\mu_i = \frac{e}{m v_{ia}} \quad (54)$$

Since  $v_{ia}$  is proportional to the partial pressure of the gas atoms  $p_a$ , according to equation (54),  $\mu_i p_a$  is a constant. Usually, the experimental values of the mobility are referred to some standard pressure and temperature (such as 1 mm Hg and 300° K), and this standard mobility is denoted  $\mu_0$ . The mobility data are then presented in curves of  $\mu_0$  against  $E/p_a$ , where  $E$  is the electric field. A set of such curves for helium, neon, and argon is presented in figure 3.24(a) of reference 25. The mobility  $\mu_0$  is nearly independent of  $E/p_a$  for low  $E/p_a$ , while it drops off with high  $E/p_a$ . Fortunately, for the effective fields  $E^*$  and gas pressures of interest here, it turns out that  $E^*/p_a$  remains in the range for which  $\mu_0$  is nearly constant.

From the preceding considerations, the ion-atom collision frequency may be written as

$$v_{ia} = \frac{e}{m} \frac{(1 - f)p}{p_{ref}} \frac{1}{\mu_0} \quad (55)$$

where  $p$  is the gas pressure in the absence of ionization,  $f$  is the degree of ionization, and  $\mu_0$  is the mobility (in units of  $m^2/(v)(\text{sec})$ ) referred to the reference pressure  $p_{ref}$ . The mobility  $\mu_0$  also decreases somewhat with increasing gas temperature, but the available data (figs. 3.25 to 3.27, ref. 25) on the temperature dependence do not go above 350° K, so this effect will not be taken into account. In any case, a smaller mobility would mean less ion slip and would result in a more optimistic estimate of the electron temperature. The values of  $\mu_0$  for helium, neon, and argon at 1 millimeter of mercury and 300° K are given in table 3.1 of reference 25. For argon,  $\mu_0$  is 0.146 square meter

per volt per second.

From equations (43) and (55), it is seen that the ion Hall parameter  $\beta_i$  is proportional to the ratio  $B/p$ . It is therefore of interest to establish the gas pressure and the magnetic field for which the maximum electron heating and the maximum power density are attained.

#### Performance of Segmented Generator with Ion Slip

Calculations were carried out for unseeded argon in a segmented electrode generator. Three magnetic-field strengths were chosen: 0.2, 2, and 10 webers per square meter. The 2-weber-per-square-meter (20,000 gauss) field is characteristic of generators that are presently in operation; a 10-weber-per-square-meter (100,000 gauss) field is also attainable. For each field strength and gas density, electron temperature, conductivity, and power density were calculated for load parameters varying between 0 and 1. From these results the value of  $K$  at which the power density reached a maximum was determined. This maximum power density, along with the corresponding conductivity and load parameter, is plotted against the reservoir pressure in figures 7 and 8. Figure 7 is for a Mach number of 3 and a stagnation temperature of  $2500^\circ\text{K}$ , for which the gas velocity is 1400 meters per second and the static temperature  $625^\circ\text{K}$ . These conditions correspond to the conditions of the previous section. Figure 8 refers to a Mach number of 1 and a stagnation temperature of  $1500^\circ\text{K}$ , for which the gas velocity is 625 meters per second and the static temperature  $1125^\circ\text{K}$ .

Several interesting conclusions can be drawn from these figures. First of all, for a given magnetic field, the power density reaches a maximum at a certain value of the gas pressure. At lower pressure, ion slip causes the power to drop off rapidly, while at higher pressures electron-atom collisions inhibit the attainment of high electron temperatures. Increasing the magnetic field raises the maximum power density considerably, but the generator must be operated at a higher gas pressure to produce the maximum power.

The effect of reducing Mach number and stagnation temperature shows up in a significant reduction in power density. This is due mostly to the smaller gas velocity. For example, comparison of the power-density curves of figures 7 and 8 shows that the maximum power density is reduced by a factor of approximately  $1/6$ . This reduction is slightly greater than the ratio of the squares of the velocities, namely,  $(625/1400)^2 \approx 1/5$ , which is the reduction expected from equation (53). Actually, because of a smaller induced electric field, the electron temperature and, therefore, the conductivity is also reduced.

The power-density data of figures 7 and 8 are plotted against  $B/p$  in figure 9 to show more clearly the operating point for maximum power output. In this figure, the ordinate is a normalized power density, obtained by dividing the actual power density by  $u^2 B^2$ , so that the normalized power density has the same units as conductivity. For a given stagnation temperature and Mach number (i.e., a given static temperature and gas velocity), the point of maximum power occurs at the same value of  $B/p$ , independent of the magnetic field. This is a consequence of the fact that  $\beta_i$  varies as  $B/p$ , while because of electron heating

$\beta_e$  is very nearly independent of  $B$ ; hence, the term  $1 + \beta_e \beta_i$  in equations (52) and (53) is a function of  $B/p$  only.

For  $T_0 = 2500^\circ \text{K}$  and  $M = 3$ , the point of maximum power occurs at  $B/p = 64$ . For  $T_0 = 1500^\circ \text{K}$  and  $M = 1$ , this point is at a lower value of  $B/p$ , namely  $B/p = 32$ . This difference arises because the lower gas velocity in the latter case results in a smaller induced electric field and lower electron temperatures.

It is interesting to note from figures 7 and 8 that the maximum conductivity and the maximum power density do not occur at the same pressures. As the gas pressure is reduced, first the power density drops off, and then the conductivity. The reason is that the generator load parameter also decreases with decreasing gas pressure, as shown by the curves for  $K$ . Thus, the conductivity is not an adequate indication of generator performance by itself. It may also be seen that the maximum power is attained for load parameters between 0.4 and 0.45, instead of 0.5, for which the factor  $K(1 - K)$  in equation (53) is a maximum.

Calculations have also been carried out for the Hall generator. The results for conductivity and power density in the Hall generator are identical to the results presented herein for the segmented electrode generator, except that the load parameter  $K$  for the segmented generator is replaced by  $1 - K_{\text{Hall}}$ , where  $K_{\text{Hall}}$  is the ratio of voltage across the terminal electrodes of the Hall generator to the open circuit voltage.

The operating pressures for maximum power density are quite reasonable; for  $B = 2$  webers per square meter, the optimum reservoir pressure is 1 atmosphere, while even for the extremely high field of  $B = 10$  webers per square meter, the optimum reservoir pressure has the reasonable value of 5 atmospheres. Since ion slip can be minimized by operating at the proper pressure, it appears that this effect need not represent any important limitation on generator performance.

#### CONCLUDING REMARKS

The calculations presented in this report indicate that very high electron temperatures, conductivities, and power densities are attainable in magnetohydrodynamic generators without seeding, and that seeding actually has a deleterious effect on electron heating. The results appear so optimistic that some reservations need to be made. First of all, it should be mentioned that this conclusion is valid only for monatomic carrier gases such as helium, neon, and argon, which have small cross sections for the elastic scattering of low-energy electrons. Of these gases, argon has the smallest cross section and is thus the most favorable for electron heating. In flame gases, which contain nondissociated molecules of water vapor, carbon dioxide, carbon monoxide, and so forth, the comparatively large cross sections for collision with electrons (about 100 times that of argon, see ref. 20) would inhibit electron heating considerably, and it is to be expected that seeding would be required to provide an acceptable degree of ionization.

A more important reservation arises from the assumption made in this report that the only mechanism of energy loss from the electrons is elastic collision with ions and atoms. Thus, it has been implicitly assumed that whatever energy the free electrons lose in inelastic collisions producing excitation or ionization of the atoms is returned to them by recombination processes. Actually, there might be a net energy loss from the free electrons due to radiative recombinations and de-excitations in which the emitted radiation escapes from the plasma. The net result of recombination could be a reduction of the electron temperature. The magnitude of this effect may be large and remains to be determined.

Lewis Research Center  
National Aeronautics and Space Administration  
Cleveland, Ohio, October 2, 1963



## APPENDIX A

### SYMBOLS

$B$	magnetic-field strength
$E$	electric field
$E^*$	effective electric field, eq. (2)
$e$	electron charge
$e_r$	electric charge of particle of $r^{\text{th}}$ species
$f$	degree of ionization
$g$	ground state degeneracy
$h$	Planck constant
$J$	current density
$K$	load parameter, eq. (21)
$K_{rt}$	defined by eq. (B3)
$k$	Boltzmann constant
$M$	Mach number
$m$	mass of gas atom
$m_r$	mass of particle of $r^{\text{th}}$ species
$N_r$	number of particles of $r^{\text{th}}$ species per unit volume
$N_r^O$	sum of number densities of ions and atoms of species $r$ , eq. (6)
$N_t$	number of particles of $t^{\text{th}}$ species per unit volume
$P$	power density
$p$	static gas pressure
$p_r$	partial pressure of $r^{\text{th}}$ species
$p_0$	stagnation or reservoir pressure
$Q$	collision cross section

$T$	static gas temperature
$T_r$	temperature of $r^{\text{th}}$ species
$T_0$	stagnation temperature
$u$	mean gas velocity, eq. (B1)
$u_r$	mean velocity of $r^{\text{th}}$ species
$V_A$	ionization potential of gas
$V_S$	ionization potential of seed
$w_r$	drift velocity of $r^{\text{th}}$ species, eq. (B4)
$w_t$	drift velocity of $t^{\text{th}}$ species
$Z_{rt}^{(11)}$	average collision cross section for momentum transfer from species $r$ to species $t$
$\alpha$	mean thermal speed, eq. (27)
$\beta_e$	electron Hall parameter, eq. (13)
$\beta_i$	ion Hall parameter, eq. (43)
$\gamma$	ratio of specific heats
$\delta$	defined by eq. (19)
$\epsilon$	defined by eq. (44)
$\epsilon_0$	permittivity of free space
$\Lambda$	defined by eq. (31)
$\mu_i$	ion mobility
$\mu_0$	reference ion mobility
$\nu_E$	effective collision frequency for energy transfer, eq. (16)
$\nu_e$	total electron collision frequency, eq. (9)
$\nu_{rt}$	mean collision frequency for momentum transfer from species $r$ to species $t$
$\rho$	total mass density
$\rho_r$	mass density of $r^{\text{th}}$ species

$\sigma_0$       electrical conductivity, eq. (12)

$\omega_e$       electron cyclotron frequency

$\omega_i$       ion cyclotron frequency

Subscripts:

A      carrier gas atom

Ar      argon

A<sup>+</sup>      carrier gas ion

a      atom

Cs      cesium

e      electron

i      ion

r      r<sup>th</sup> species (r = e, i, a, A, A<sup>+</sup>, S, S<sup>+</sup>)

ref      reference

S      seed atom

S<sup>+</sup>      seed ion

t      t<sup>th</sup> species (t = e, i, a, A, A<sup>+</sup>, S, S<sup>+</sup>)

x, y      coordinate directions

Superscript:

→      vector

## APPENDIX B

### SIMPLIFICATION OF BURGERS' MOMENTUM AND ENERGY EQUATIONS

The assumptions that are used in the reduction and simplification of Burgers' momentum and energy equations are discussed herein. Reference 13 may be consulted for the general method of deriving these equations and for their application to the calculation of the transport properties of gases.

It is assumed that the distribution function of each species is nearly Maxwellian with respect to the mean gas velocity, which is defined as

$$\rho \vec{u} = \sum_r \rho_r \vec{u}_r \quad (B1)$$

where  $\rho$  is the mass density of species  $r$  and  $\rho$  is the total density, that is,  $\rho = \sum_r \rho_r$ . The mean velocity of the  $r^{\text{th}}$  species is denoted by  $\vec{u}_r$ .

The distribution function is written as the sum of the Maxwellian distribution and a small perturbation (see eq. 52, ref. 13). Because of the assumed smallness of the perturbation, its contribution to the transfer equations is of importance only when it appears in terms with large coefficients. The collision terms contain the collision frequencies as coefficients, and since these frequencies are large (of the order of  $10^{10}$ /sec) in the cases of interest in this report, the contribution of the perturbation must be retained in the collision terms. Furthermore, since strong electric and magnetic fields are to be considered herein, coefficients containing the intensities of these fields are also large. An example of such a coefficient is the electron cyclotron frequency  $eB/m_e$ , which for the magnetic-field strengths of interest is of the order of  $10^{11}$  per second. Section 6, page 25, of reference 13 contains a more complete discussion of this method of treating the perturbation terms.

The resulting equation for the transfer of momentum from species  $r$  may be written as

$$\begin{aligned} \rho_r (\vec{u} \cdot \nabla) \vec{u} + \nabla p_r - N_r e_r (\vec{E}^* + \vec{w}_r \times \vec{B}) \\ = - \sum_t N_r \frac{m_r m_t}{m_r + m_t} \nu_{rt} \left[ (\vec{w}_r - \vec{w}_t) - \frac{z_{rt}}{m_r + m_t} (m_t \vec{r}_r - m_r \vec{r}_t) \right] \end{aligned} \quad (B2)$$

The left side of equation (B2) is taken from the expression 56 on page 30 of reference 13. Here, steady-state conditions are assumed, the gravity force is neglected, and the intensity  $B$  of the magnetic field is expressed in mks units. The collision term appearing on the right side is identical to expression 83 on

page 42 of reference 13, except that Burgers' "friction coefficient"  $K_{rt}$  has been related to the collision frequency  $\nu_{rt}$  for momentum transfer from species  $r$  to species  $t$  by the equality

$$K_{rt} = \frac{m_r m_t}{m_r + m_t} N_r \nu_{rt} \quad (B3)$$

where  $N_r$  is the number of particles of species  $r$  per unit volume. In equation (B2),  $p_r$  stands for the partial pressure of the  $r^{\text{th}}$  species,  $e_r$  is the electric charge of a particle of the  $r^{\text{th}}$  species,  $\vec{w}_r$  is the drift velocity, of this species relative to the mean flow velocity, that is,

$$\vec{w}_r = \vec{u}_r - \vec{u} \quad (B4)$$

and  $\vec{E}^*$  stands for the effective electric field in a coordinate system moving with the mean gas velocity:

$$\vec{E}^* = \vec{E} + \vec{u} \times \vec{B} \quad (B5)$$

The coefficient  $z_{rt}$  is the ratio of two cross sections (see eq. 81, ref. 13) and is usually of order unity. The vectors  $\vec{r}_r$  and  $\vec{r}_t$  are reduced heat flux vectors (defined in eq. 82, ref. 13). They will be neglected here. Their neglect corresponds to the so-called first approximation for the diffusion coefficients. The second approximation is obtained by including them. Actually, calculations using this second approximation have been carried out by the authors along the lines of the analysis of reference 26 for a partially ionized gas. Such calculations are rather lengthy and are not included in this report. The second approximation leads to more optimistic values of the conductivity and the power density in an MHD generator, however. (The maximum increase in conductivity was about 6 percent, and the maximum increase in power density was about 17 percent for a segmented electrode generator operating with unseeded argon at Mach 3 with a magnetic field of 2 webers/sq m, a stagnation temperature of 2500° K and a stagnation pressure of 3 atm.)

The equation for the transfer of energy from species  $r$  may be written as

$$\frac{3}{2} \vec{u} \cdot \nabla p_r + \frac{5}{2} p_r (\nabla \cdot \vec{u}) - N_r e_r \vec{w}_r \cdot \vec{E}^* = - \sum_t 3N_r \frac{m_r m_t}{(m_r + m_t)^2} \nu_{rt} k (T_r - T_t) \quad (B6)$$

where  $k$  is the Boltzmann constant. The left side of equation (B6) is expression 59, page 31, of reference 13, while the collision term on the right side follows from expression 99, page 50, of reference 13.

Because of the mass factor  $m_r m_t / (m_r + m_t)^2$  on the right side of equation (B6), the rate of energy transfer by elastic collisions between the atom and the ion species is much larger than the rate of energy transfer in elastic

collisions between the electrons and the atoms or the ions. Thus, it may be expected that collisions between ions and atoms will tend to maintain temperature equilibrium between them, whereas the electron temperature may greatly exceed the temperatures of the ions and the atoms. For this reason it will be assumed that the temperatures of the ion and the atom species are the same as the static temperature  $T$  of the gas mixture (excluding the electrons), that is,

$$T_t = T \quad \text{for } t \neq e \quad (B7)$$

The gas temperature  $T$  will be assumed to be known. As a result of these assumptions the only energy equation that need be considered is that for the electrons.

The inertia terms in the momentum equations for the ions and the electrons (but not for the atoms) will be neglected. To provide some justification for neglecting these terms, the following argument is given: A three-component plasma consisting of electrons (e), ions (i), and atoms (a) is considered. The argument may be easily extended to a seeded plasma having two atom and two ion species. Equations (B2) are written

$$\rho_e(\vec{u} \cdot \nabla)\vec{u} + \nabla p_e + N_e e(\vec{E}^* + \vec{w}_e \times \vec{B}) = \vec{M}_{ei} + \vec{M}_{ea} \quad (B8)$$

$$\rho_i(\vec{u} \cdot \nabla)\vec{u} + \nabla p_i - N_i e(\vec{E}^* + \vec{w}_i \times \vec{B}) = \vec{M}_{ie} + \vec{M}_{ia} \quad (B9)$$

$$\rho_a(\vec{u} \cdot \nabla)\vec{u} + \nabla p_a = \vec{M}_{ae} + \vec{M}_{ai} \quad (B10)$$

The collision terms for momentum transfer from species  $r$  to species  $t$  are here abbreviated as  $\vec{M}_{rt}$ . Note that

$$\vec{M}_{rt} = -\vec{M}_{tr} \quad (B11)$$

Since  $\rho_e \ll \rho_a$ , the electron inertia term  $\rho_e(\vec{u} \cdot \nabla)\vec{u}$  is clearly much smaller than the atom inertia term  $\rho_a(\vec{u} \cdot \nabla)\vec{u}$ . According to equation (B10),  $|\rho_a(\vec{u} \cdot \nabla)\vec{u}|$  is of the same order as  $|\vec{M}_{ae}| = |\vec{M}_{ea}|$ . Thus,  $|\rho_e(\vec{u} \cdot \nabla)\vec{u}| \ll |\vec{M}_{ea}|$ , and the electron inertia term in equation (B8) may be neglected. If it is assumed that the gas is only slightly ionized, then  $\rho_i \ll \rho_a$ . A similar argument using equations (B9) and (B10) may be made to justify neglecting the ion inertia term.

The ion pressure gradient  $\nabla p_i$  will also be assumed small in comparison with the electron and the atom pressure gradients because of the low degree of ionization and the high electron temperature. Therefore, the momentum equations (B8) and (B9) are simplified to

$$\nabla p_e + N_e e(\vec{E}^* + \vec{w}_e \times \vec{B}) = \vec{M}_{ei} + \vec{M}_{ea} \quad (B12)$$

$$- N_i e(\vec{E}^* + \vec{w}_i \times \vec{B}) = \vec{M}_{ie} + \vec{M}_{ia} \quad (B13)$$

In the electron energy equation, two terms involving gradients appear, namely,  $\frac{3}{2} \vec{u} \cdot \nabla p_e$  and  $\frac{5}{2} p_e (\nabla \cdot \vec{u})$ . The assumption that the gas is only slightly ionized may be utilized to show that  $\frac{3}{2} \vec{u} \cdot \nabla p_e \gg \frac{5}{2} p_e (\nabla \cdot \vec{u})$ . This argument proceeds as follows: The continuity equation for the gas mixture is

$$\nabla \cdot (\rho \vec{u}) = 0 \quad (\text{B14})$$

from which it follows that

$$\nabla \cdot \vec{u} = -\vec{u} \cdot \frac{\nabla \rho}{\rho} \quad (\text{B15})$$

Since  $\rho_e$  and  $\rho_i$  are assumed to be much smaller than  $\rho_a$ , the approximation  $\rho \approx \rho_a$  may be made in equation (B15). The following approximation is then obtained:

$$\frac{5}{2} p_e (\nabla \cdot \vec{u}) \approx -\frac{5}{2} p_e \vec{u} \cdot \left( \frac{\nabla N_a}{N_a} \right) \quad (\text{B16})$$

The term  $\frac{3}{2} \vec{u} \cdot \nabla p_e$  is written as

$$\frac{3}{2} \vec{u} \cdot \nabla p_e = \frac{3}{2} p_e \vec{u} \cdot \left( \frac{\nabla N_e}{N_e} + \frac{\nabla T_e}{T_e} \right) \quad (\text{B17})$$

If the gradients  $\nabla N_e$  and  $\nabla N_a$  are assumed to be of the same order,<sup>4</sup> then because of the assumption of slight ionization,  $N_a \gg N_e$ , comparison of expressions (B16) and (B17) leads to the conclusion that  $\frac{3}{2} \vec{u} \cdot \nabla p_e \gg \frac{5}{2} p_e (\nabla \cdot \vec{u})$ .

Therefore, the electron energy equation may be written as

$$\frac{3}{2} \vec{u} \cdot \nabla p_e + N_e e \vec{w}_e \cdot \vec{E}^* = -\frac{3}{2} N_e k (T_e - T) \sum_{t \neq e} \frac{2m_e}{m_t} \nu_{et} \quad (\text{B18})$$

where  $m_e$  has been neglected in the sum  $m_e + m_t$  on the right side of equation (B6).

The electron pressure gradient appears in equations (B12) and (B18). It will be assumed that within the generator duct there is a section at which the electron temperature and electron number density together attain a maximum;

---

<sup>4</sup>If the ions did not diffuse away from the region where they were produced, the relation  $N_i + N_a = N_a^0 = \text{constant}$  might be expected to be valid at each point ( $N_a^0$  is the initial atom number density before ionization takes place). Since  $N_e = N_i$  by charge neutrality, the preceding relation would imply  $\nabla N_e = -\nabla N_a$ .

hence, the pressure gradient  $\nabla p_e$  is negligibly small. The present analysis is restricted to this region. Clearly, the assumption that the electron temperature and number density are at their maximum attainable values will result in the most optimistic estimate of generator performance.

## REFERENCES

1. Steg, Leo, and Sutton, George W.: The Prospects of MHD Power Generation. *Astronautics*, vol. 5, no. 8, Aug. 1960, pp. 22-25; 82-85.
2. Brogan, T. R., Kantrowitz, A. R., Rosa, R. J., and Stekly, Z. J. J.: Progress in MHD Power Generation. *Engineering Aspects of Magnetohydrodynamics*, Clifford Mannal and Norman W. Mather, eds., Columbia Univ. Press, 1962, pp. 147-165.
3. Way, S.: Comparison of Theoretical and Experimental Results in an MHD Generator. *Engineering Aspects of Magnetohydrodynamics*, Clifford Mannal and Norman W. Mather, eds., Columbia Univ. Press, 1962, pp. 166-179.
4. Blackman, Vernon H., Jones, Malcolm S., Jr., and Demetriades, Anthony: MHD Power-Generation Studies in Rectangular Channels. *Engineering Aspects of Magnetohydrodynamics*, Clifford Mannal and Norman W. Mather, eds., Columbia Univ. Press, 1962, pp. 180-210.
5. Kennard, Earle H.: *Kinetic Theory of Gases*. McGraw-Hill Book Co., Inc., 1938.
6. Compton, K. T.: On the Motions of Electrons in Gases. *Phys. Rev.*, vol. 22, Oct. 1923, pp. 333-346.
7. Kerrebrock, Jack L.: Conduction in Gases with Elevated Electron Temperature. *Engineering Aspects of Magnetohydrodynamics*, Clifford Mannal and Norman W. Mather, eds., Columbia Univ. Press, 1962, pp. 327-346.
8. Zemansky, Mark W.: *Heat and Thermodynamics*. Third ed., McGraw-Hill Book Co., Inc., 1951, p. 412.
9. Ben Daniel, D. J., and Tamor, S.: Nonequilibrium Ionization in Magnetohydrodynamic Generators. Rep. 62-RL-(2922-E), General Electric Co., Jan. 1962.
10. Hurwitz, H., Jr., Sutton, G. W., and Tamor, S.: Electron Heating in Magnetohydrodynamic Power Generators. *ARS Jour.*, vol. 32, no. 8, Aug. 1962, pp. 1237-1243.
11. Wright, J. K., and Swift-Hook, D. T.: Magnetohydrodynamic Generation with Elevated Electron Temperature. *Proc. Phys. Soc.*, pt. 2, vol. 80, no. 514, 1962, pp. 465-471.
12. Dougal, A. A., and Goldstein, L.: Energy Exchange Between Electron and Ion Gases Through Coulomb Collisions in Plasmas. *Phys. Rev.*, vol. 109, no. 3, Feb. 1, 1958, pp. 615-624.

13. Burgers, J. M.: Selected Topics from the Theory of Gas Flow at High Temperatures. Ch. V. The Application of Transfer Equations to the Calculation of Diffusion, Heat Conduction, Viscosity and Electric Conductivity. Tech. Notes BN-124a; b, Inst. for Fluid Dynamics and Appl. Math., Univ. Maryland, May 1958.
14. Burgers, J. M.: Statistical Plasma Mechanics. Ch. 5 of Symposium on Plasma Dynamics, Francis H. Clauser, ed., Addison-Wesley Pub. Co., Inc., 1960.
15. Rouse, Carl A.: Ionization-Equilibrium Equation of State. Pt. II. Mixtures. Astrophysical Jour., vol 135, no. 2, Mar. 1962, pp. 599-615.
16. Fay, J. A.: Electrical Conductivity of Combustion Gases. Engineering Magnetohydrodynamics, M.I.T., June 19-30, 1961, pp. 3.4-1-3.4-9.
17. Herdan, R., and Liley, B. S.: Dynamical Equations and Transport Relationships for a Thermal Plasma. Rev. Modern Phys., vol. 32, no. 4, Oct. 1960, pp. 731-741.
18. Frost, L. S., and Phelps, A. V.: Momentum Transfer Cross Section for Electrons in Argon. Bull. Am. Phys. Soc., ser. II, vol. 5, no. 5, 1960, p. 371.
19. Chen, C. L., and Raether, M.: Collision Cross Section of Slow Electrons and Ions with Cesium Atoms. Phys. Rev., vol. 128, no. 6, Dec. 15, 1962, pp. 2679-2683.
20. Dibelius, N. R., Luebke, E. A., and Mullaney, G. J.: Electrical Conductivity of Flame Gases Seeded with Alkali Metals and Application to MHD Powerplant Design. Engineering Aspects of Magnetohydrodynamics, Clifford Mannal and Norman W. Mather, eds., Columbia Univ. Press, 1962, pp. 307-326.
21. Brode, R. B.: The Absorption Coefficient for Slow Electrons in Alkali Metal Vapors. Phys. Rev., vol. 34, no. 5, Sept. 1, 1929, pp. 673-678.
22. Flavin, R. K., and Meyerand, R. G., Jr.: Collision Probability of Low Energy Electrons with Cesium Atoms. Advanced Energy Conversion, vol. 3, no. 1, Jan.-Mar. 1963, pp. 3-18.
23. Robinson, Lawrence Baylor: Theoretical Collision Frequency Between Electrons and Neutral Atoms in a Cesium Plasma. Phys. Rev., vol. 127, no. 6, Sept. 15, 1962, pp. 2076-2080.
24. Rosa, Richard J.: Physical Principles of Magnetohydrodynamic Power Generation. Phys. of Fluids, vol. 4, no. 2, Feb. 1961, pp. 182-194.
25. Brown, Sanborn C.: Basic Data of Plasma Physics. Technology Press, M.I.T., 1959.
26. Pipkin, A. C.: Electrical Conductivity of Partially Ionized Gases. Phys. of Fluids, vol. 4, no. 1, Jan. 1961, pp. 154-158.

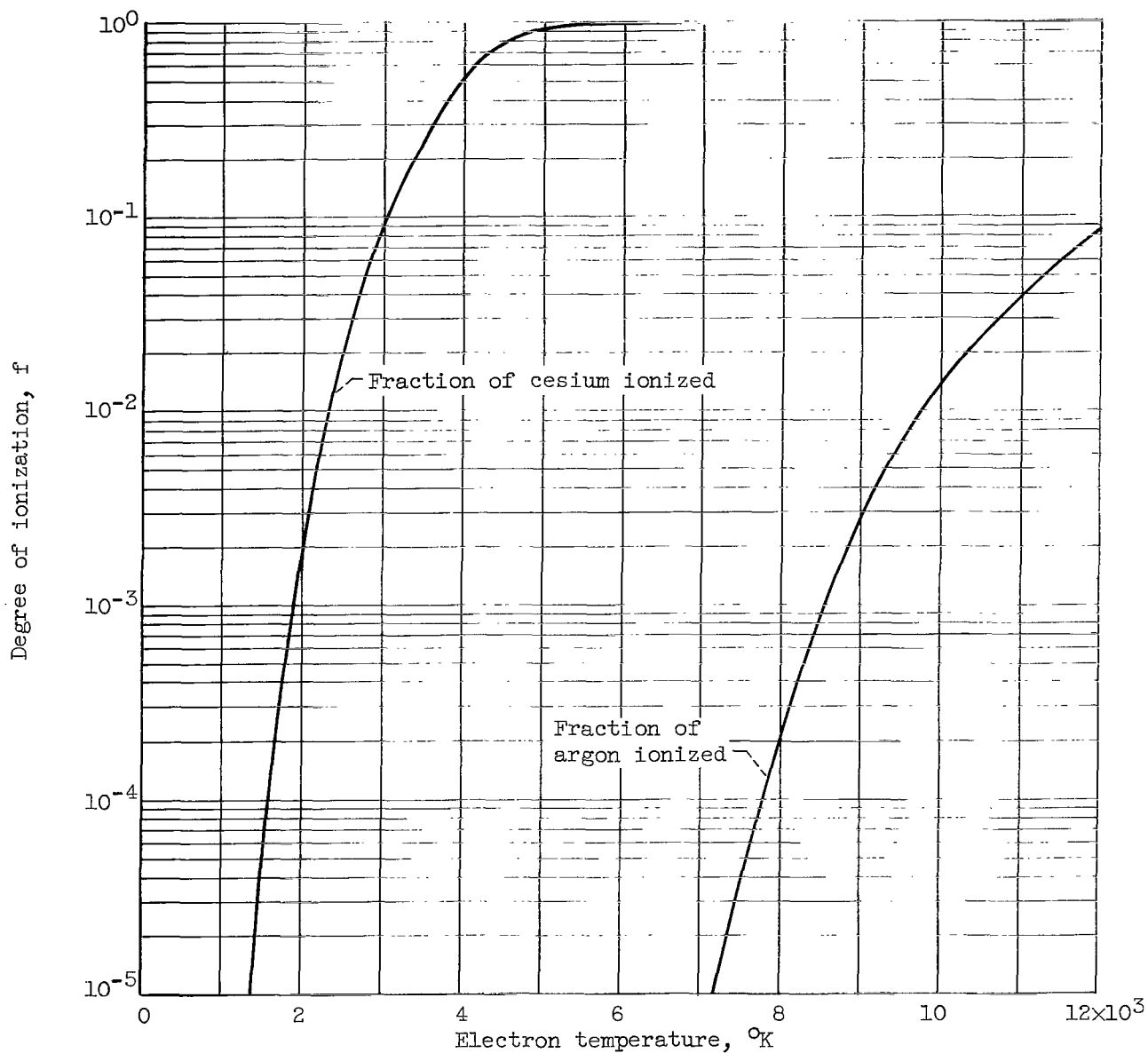


Figure 1. - Degrees of ionization of constituents of seeded plasma for various electron temperatures. Argon with 1-percent cesium seed; initial argon number density,  $1.1 \times 10^{18}$  per cubic centimeter.

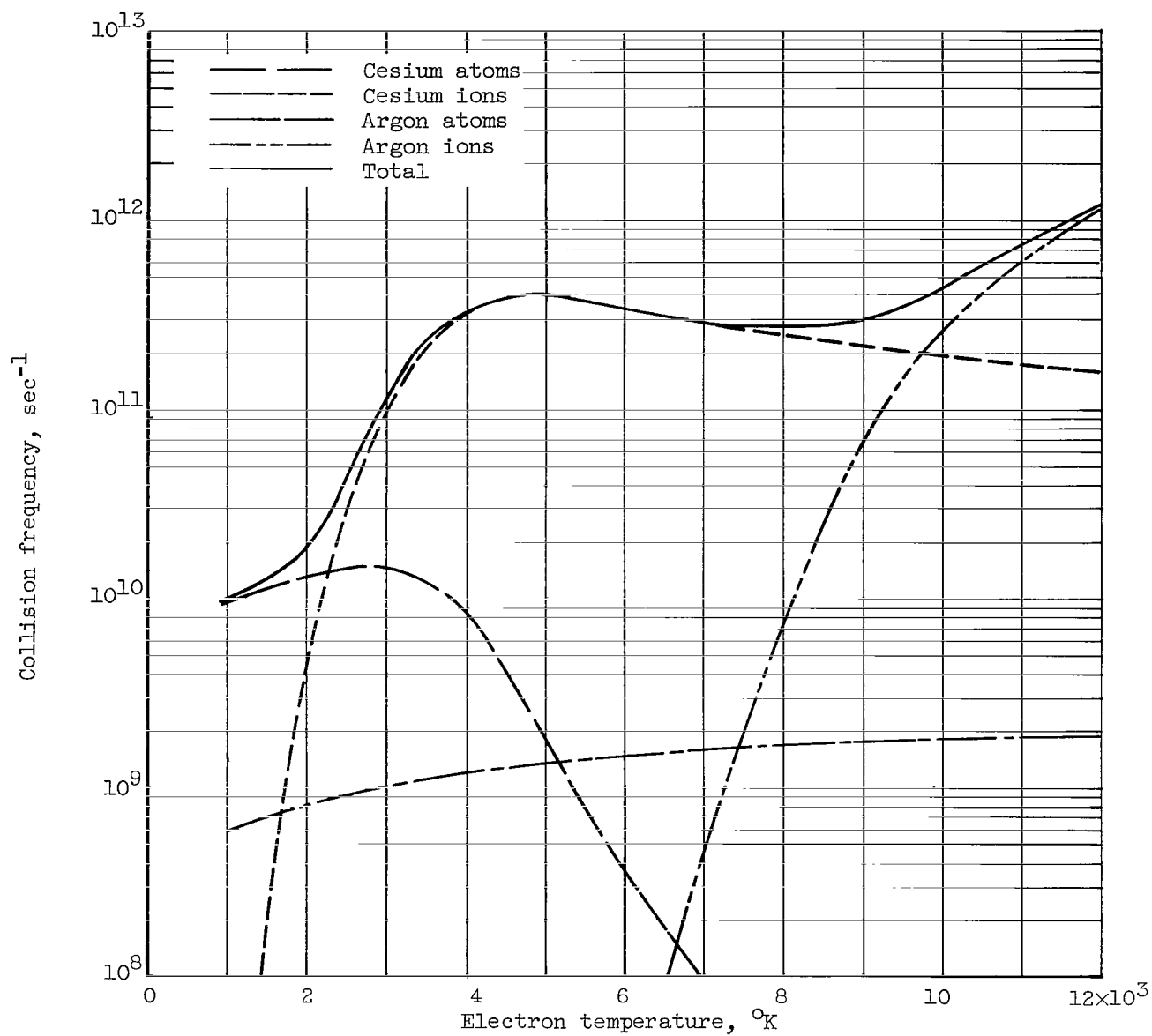
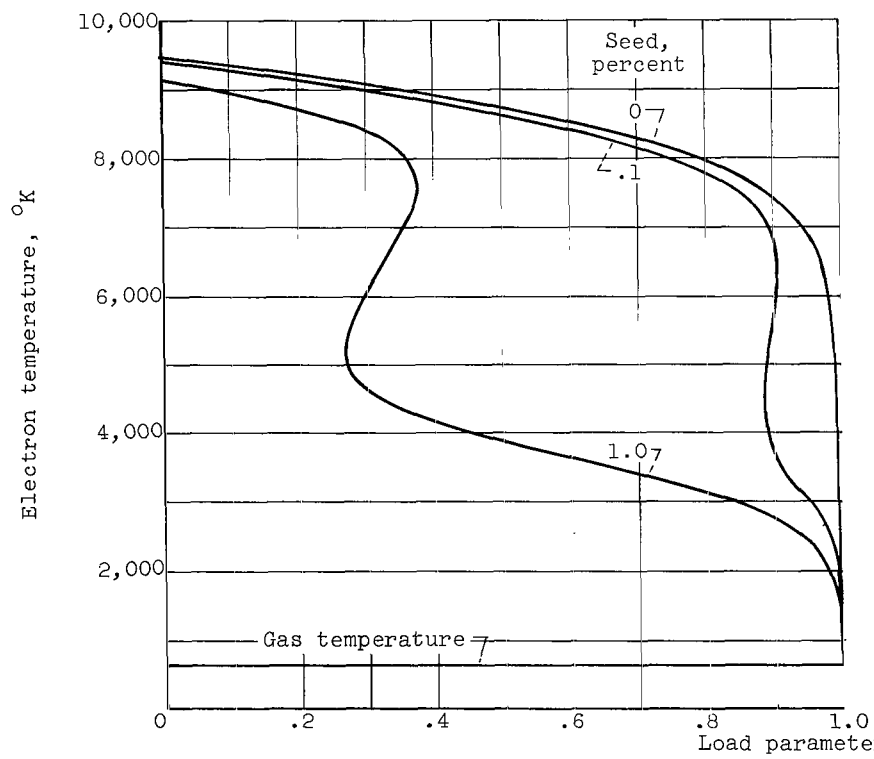
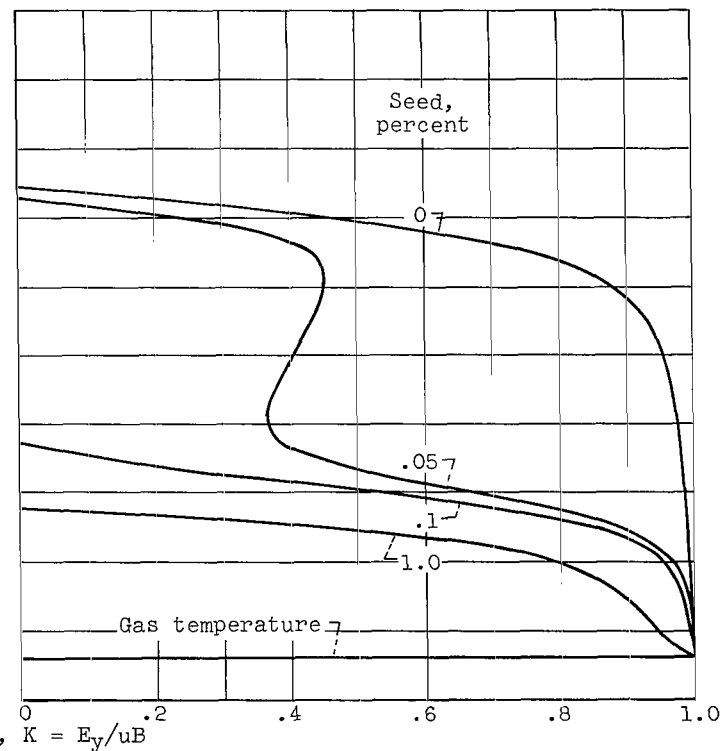


Figure 2. - Collision frequency as function of electron temperature for seeded plasma. Argon with 1-percent cesium seed; initial argon number density,  $1.1 \times 10^{18}$  per cubic centimeter.

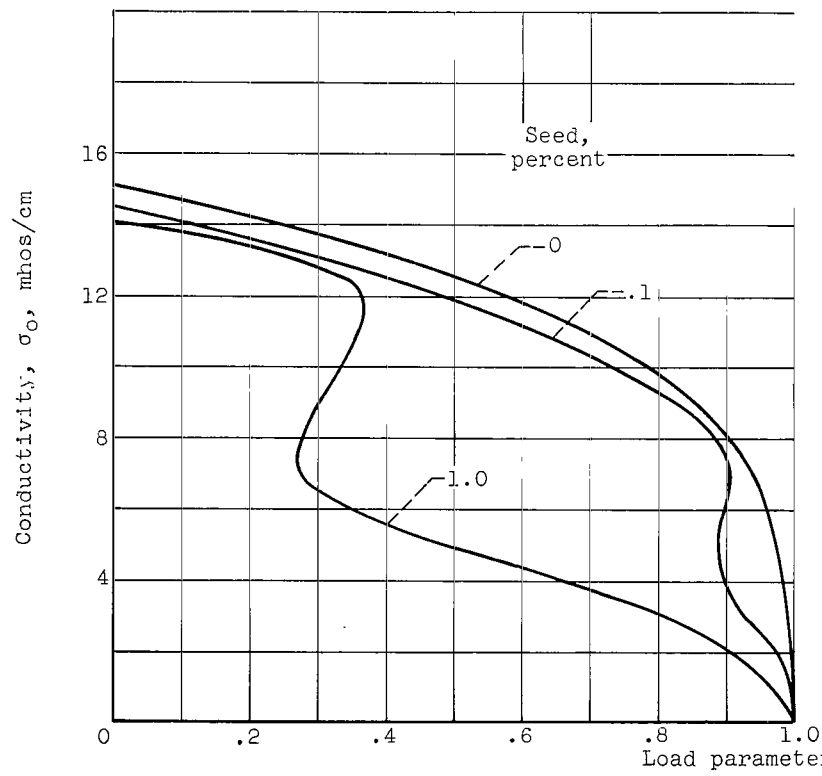


(a) Magnetic-field strength, 2 webers per square meter.

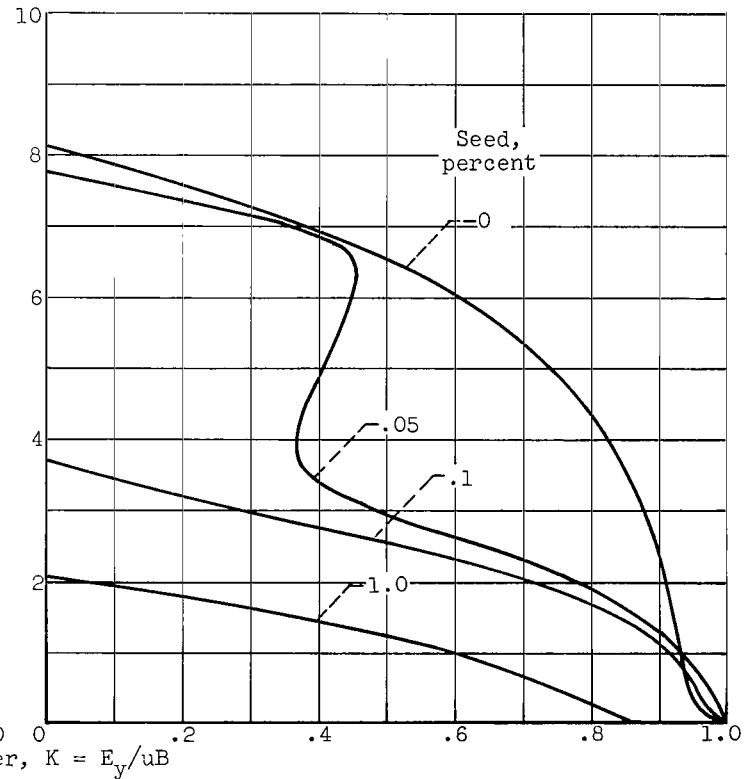


(b) Magnetic-field strength, 0.2 webers per square meter.

Figure 3. - Electron temperature as function of load parameter. Segmented electron generator; argon seeded with cesium; stagnation pressure, 3 atmospheres; stagnation temperature, 2500° K; Mach number, 3; static gas temperature, 625° K; mean gas velocity, 1400 meters per second.



(a) Magnetic-field strength, 2 webers per square meter.



(b) Magnetic-field strength, 0.2 webers per square meter.

Figure 4. - Conductivity as function of load parameter. Segmented electrode generator; argon seeded with cesium; stagnation pressure, 3 atmospheres; stagnation temperature, 2500° K; Mach number, 3; static gas temperature, 625° K; mean gas velocity, 1400 meters per second.

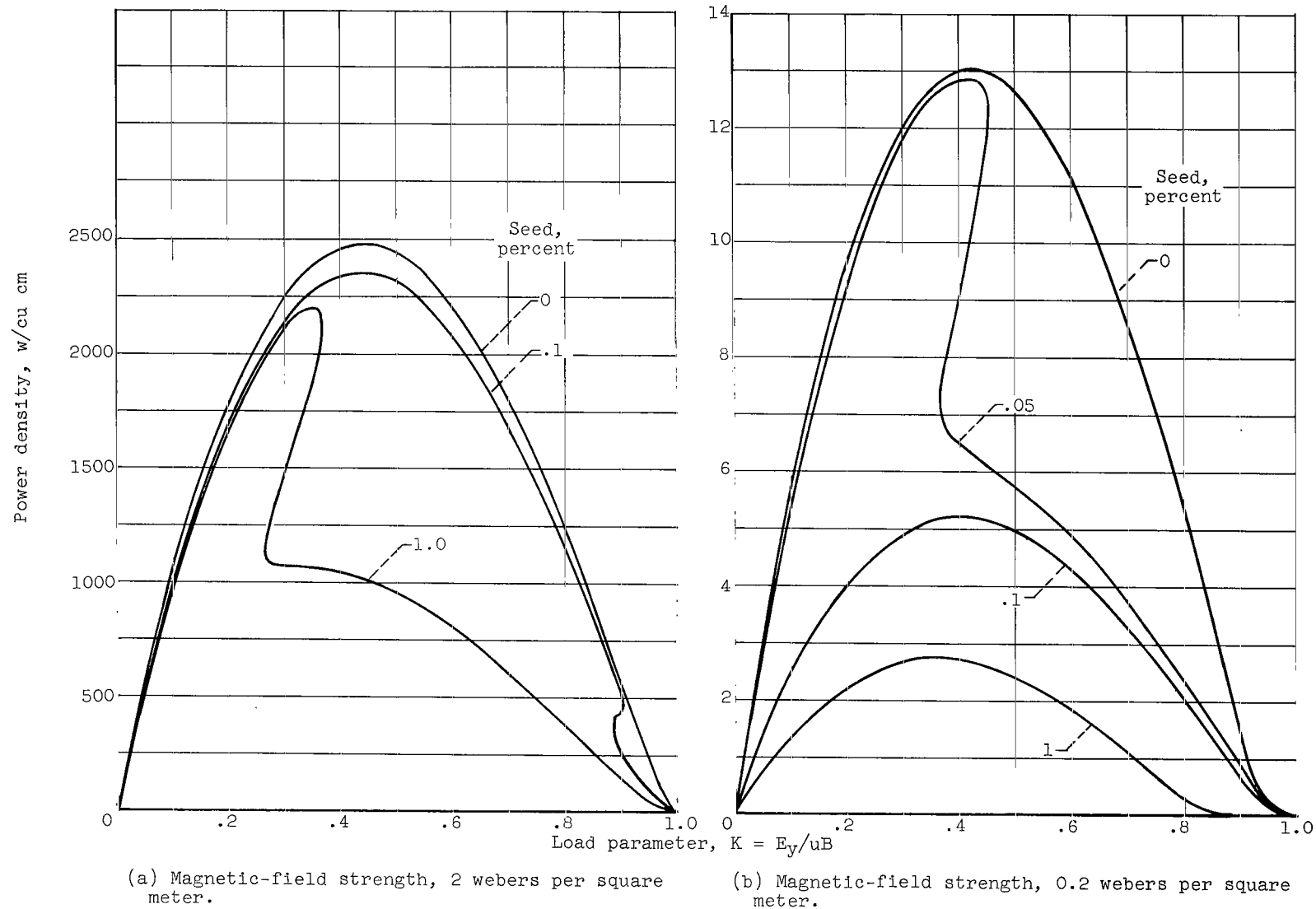


Figure 5. - Power density as function of load parameter. Segmented electrode generator; argon seeded with cesium; stagnation pressure, 3 atmospheres; stagnation temperature, 2500° K; Mach number, 3; static gas temperature, 625° K; mean gas velocity, 1400 meters per second.

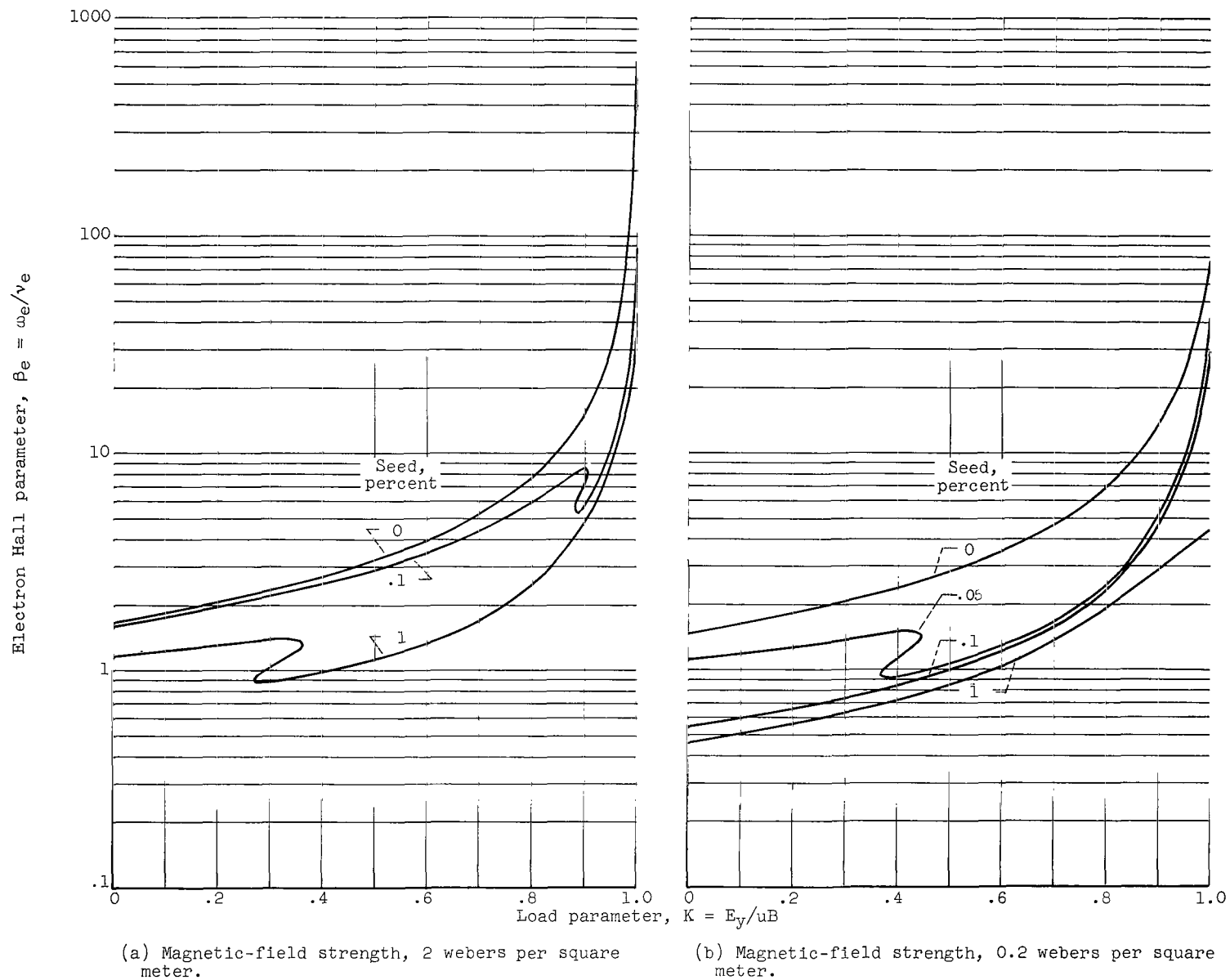
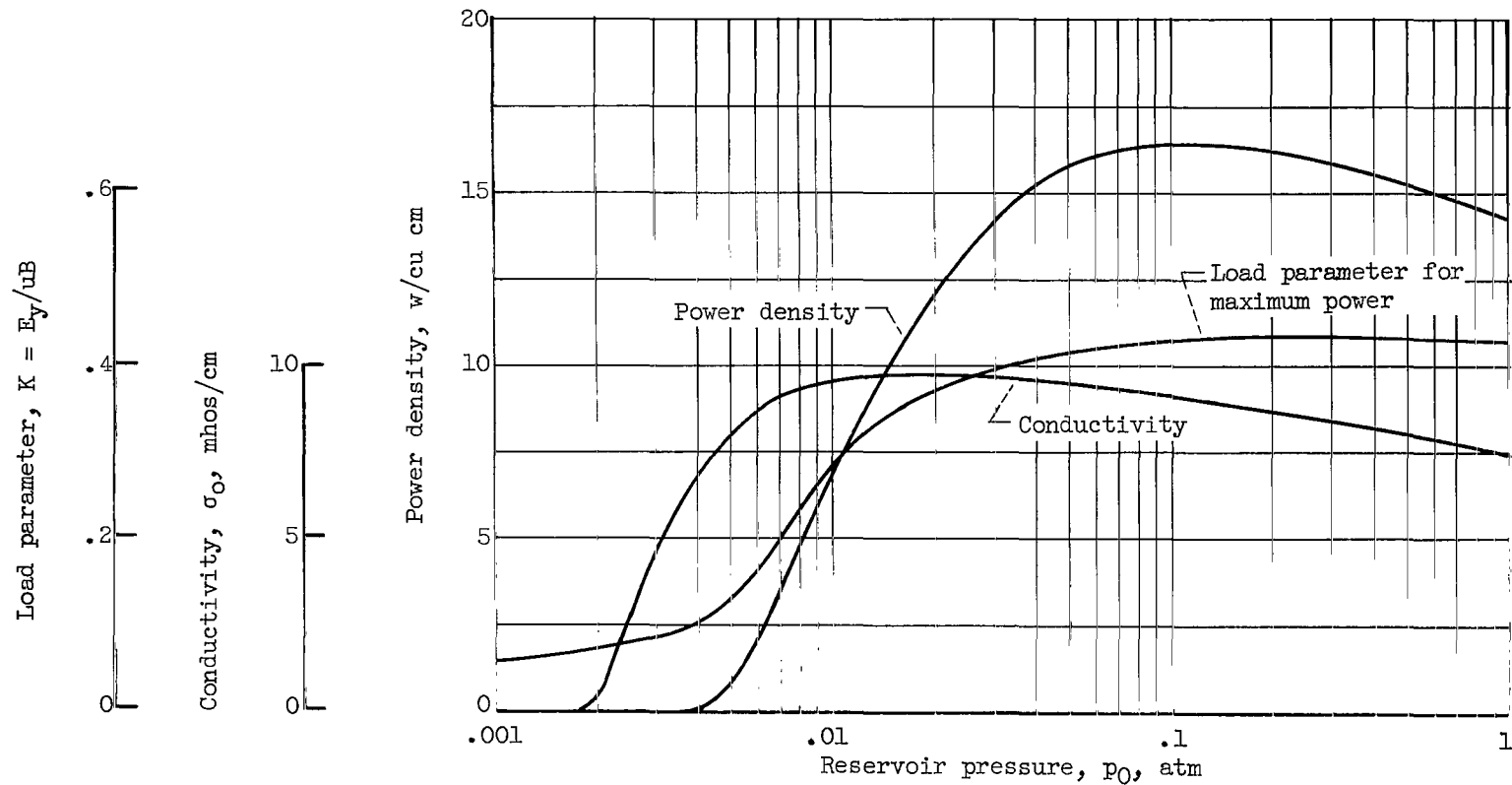
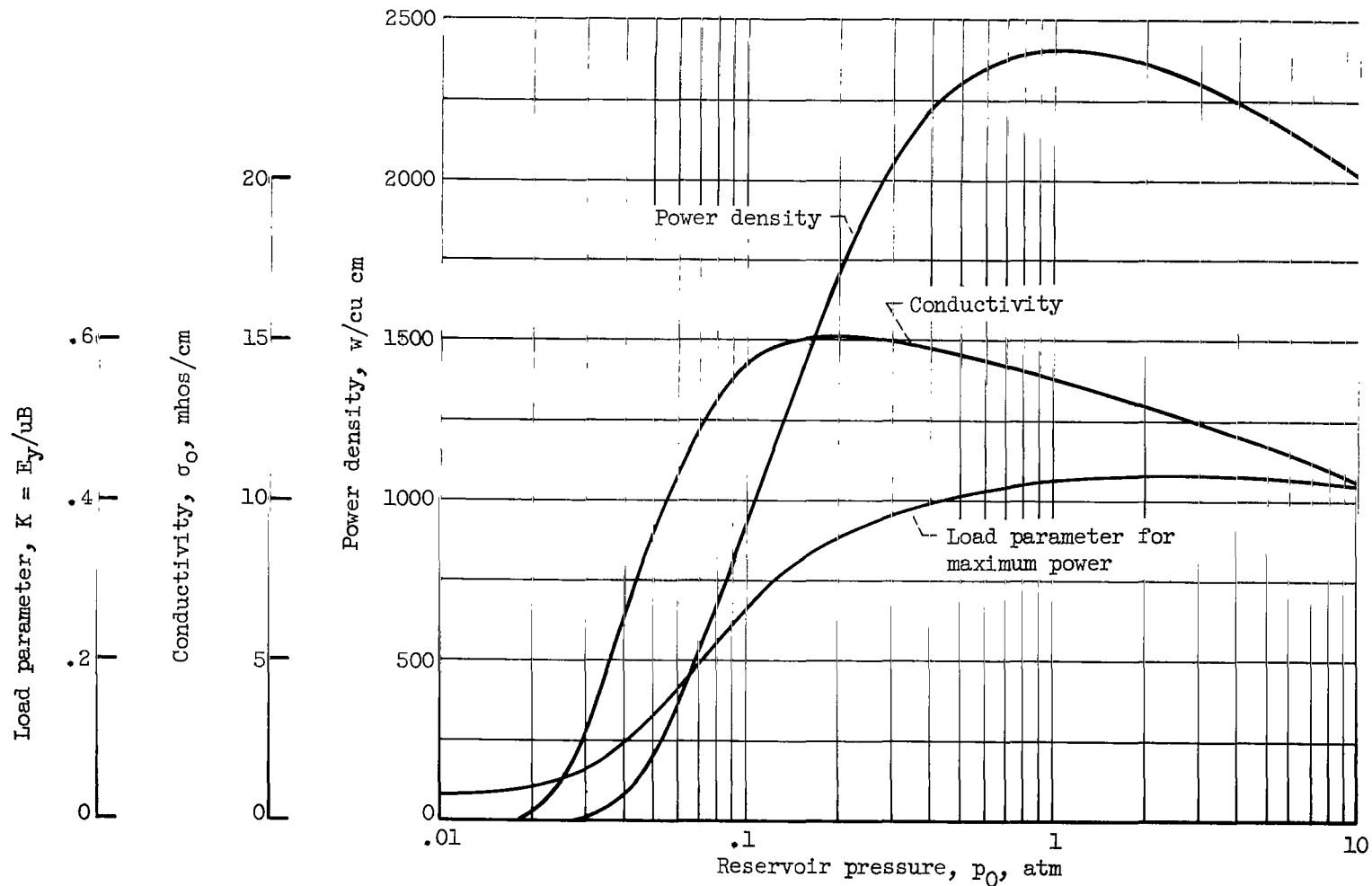


Figure 6. - Hall parameter as function of load parameter. Segmented electrode generator; argon seeded with cesium; stagnation pressure, 3 atmospheres; stagnation temperature, 2500° K; Mach number, 3; static gas temperature, 625° K; mean gas velocity, 1400 meters per second.



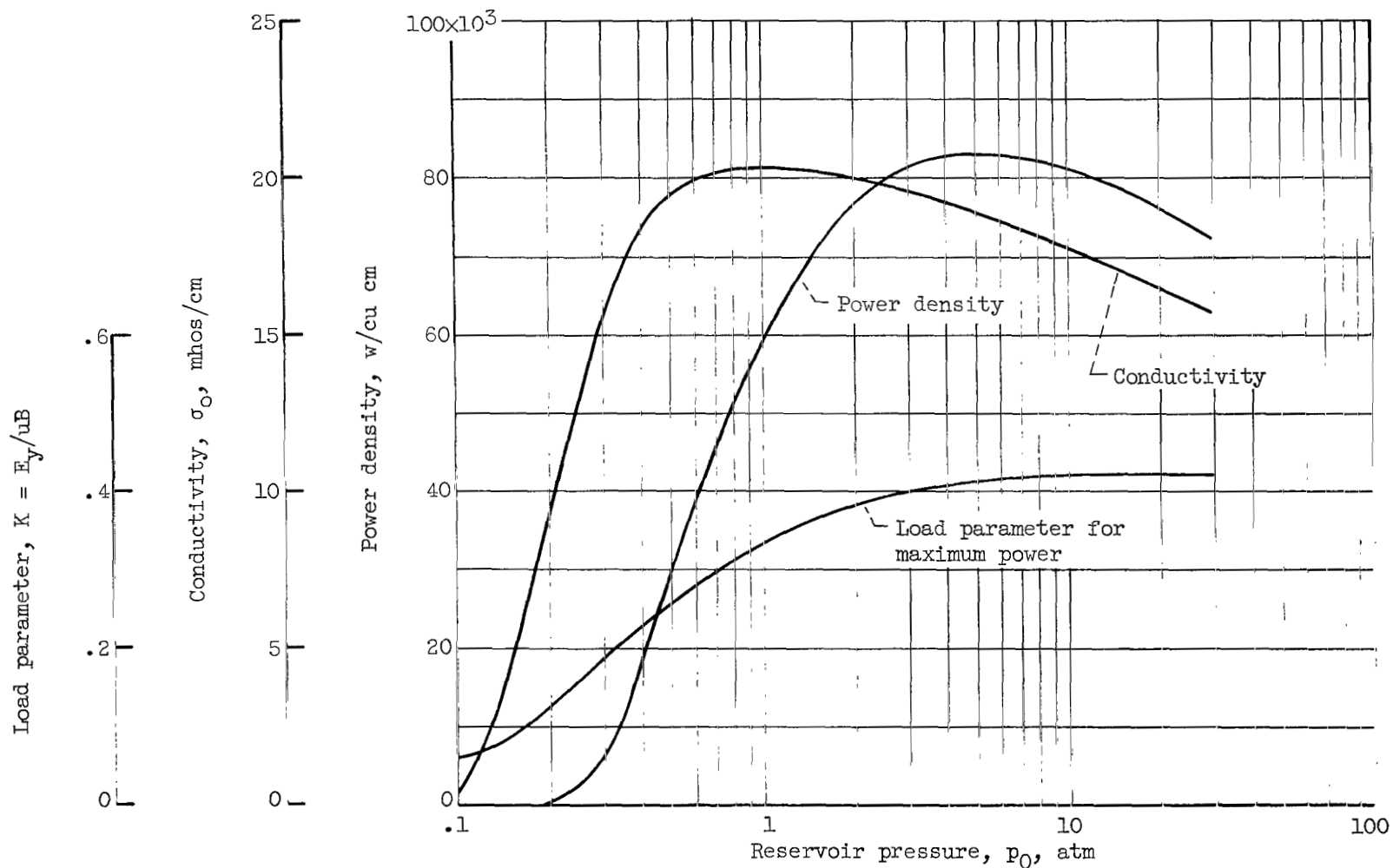
(a) Magnetic-field strength, 0.2 weber per square meter.

Figure 7. - Effect of reservoir pressure on generator performance for unseeded argon. Stagnation temperature,  $2500^\circ \text{K}$ ; Mach number, 3; static gas temperature,  $625^\circ \text{K}$ ; mean gas velocity, 1400 meters per second.



(b) Magnetic-field strength, 2 webers per square meter.

Figure 7. - Continued. Effect of reservoir pressure on generator performance for unseeded argon. Stagnation temperature,  $2500^\circ \text{K}$ ; Mach number, 3; static gas temperature,  $625^\circ \text{K}$ ; mean gas velocity, 1400 meters per second.



(c) Magnetic-field strength, 10 webers per square meter.

Figure 7. - Concluded. Effect of reservoir pressure on generator performance for unseeded argon. Stagnation temperature,  $2500^\circ \text{K}$ ; Mach number, 3; static gas temperature,  $625^\circ \text{K}$ ; mean gas velocity, 1400 meters per second.

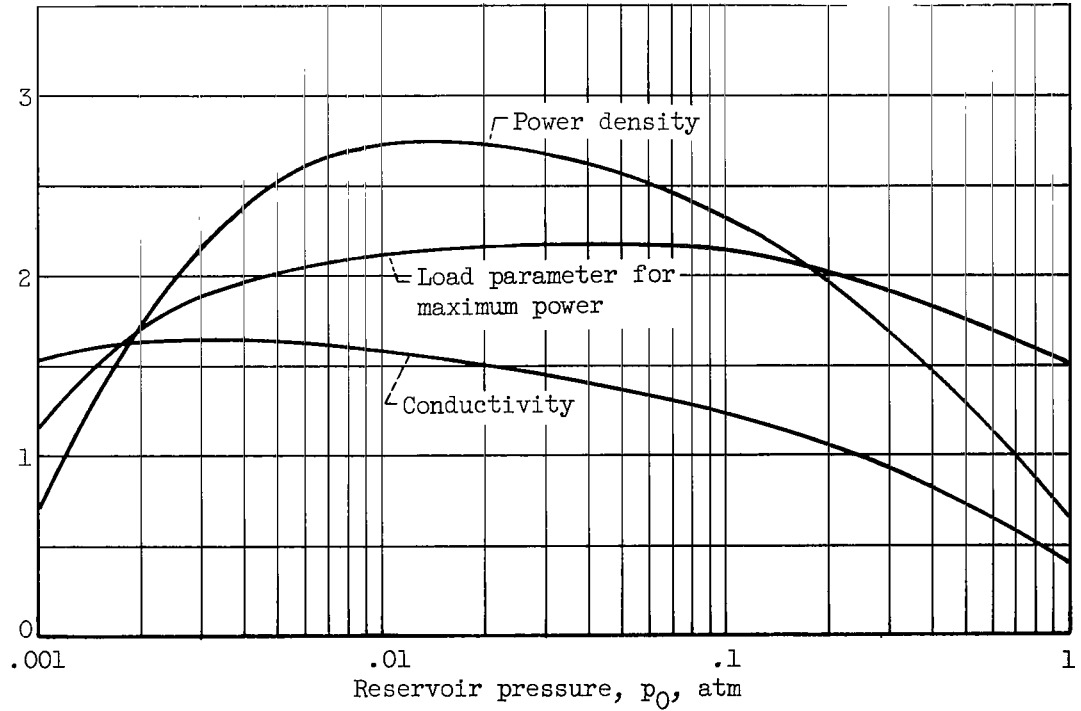
Load parameter,  $K = E_y / uB$

.6  
.4  
.2  
0

Conductivity,  $\sigma_0$ , mhos/cm

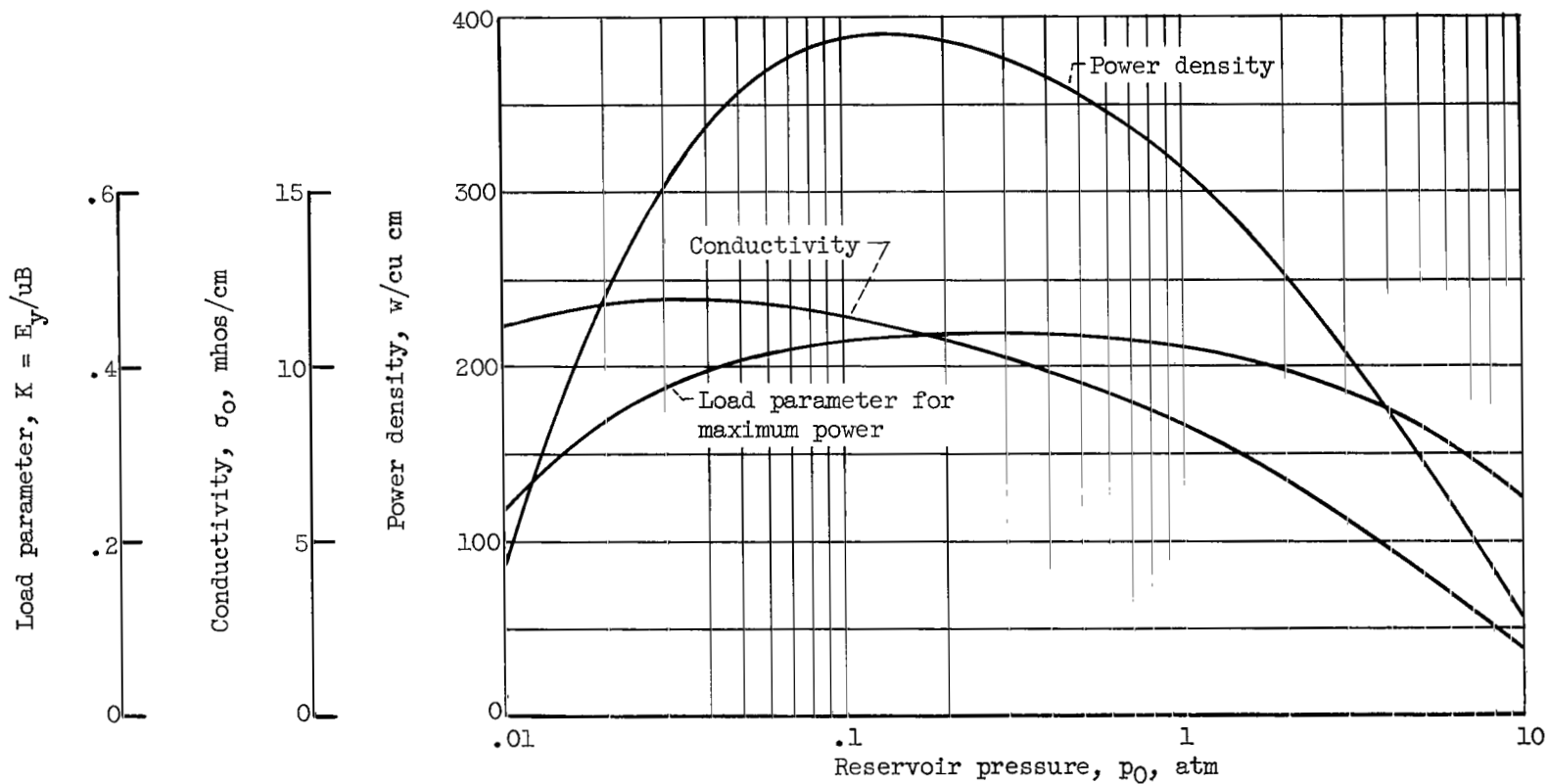
10  
5  
0

Power density,  $w/cu\text{ cm}$



(a) Magnetic-field strength, 0.2 weber per square meter.

Figure 8. - Effect of reservoir pressure on generator performance for unseeded argon. Stagnation temperature,  $1500^\circ\text{K}$ ; Mach number, 1; static gas temperature,  $1125^\circ\text{K}$ ; mean velocity, 625 meters per second.



(b) Magnetic-field strength, 2 webers per square meter.

Figure 8. - Continued. Effect of reservoir pressure on generator performance for unseeded argon. Stagnation temperature,  $1500^\circ\text{K}$ ; Mach number, 1; static gas temperature,  $1125^\circ\text{K}$ ; mean gas velocity, 625 meters per second.

Load parameter,  $K = E_y/uB$

.6  
.4  
.2  
0

Conductivity,  $\sigma_0$ , mhos/cm

20  
15  
10  
5  
0

Power density,  $w$ , w/cu cm

$16 \times 10^3$   
12  
8  
4  
0

.01

.1

1

10

Reservoir pressure,  $p_0$ , atm

Conductivity

Power density

Load parameter for maximum power

(c) Magnetic-field strength, 10 webers per square meter.

Figure 8. - Concluded. Effect of reservoir pressure on generator performance for unseeded argon. Stagnation temperature,  $1500^\circ \text{K}$ ; Mach number, 1; static gas temperature,  $1125^\circ \text{K}$ ; mean gas velocity, 625 meters per second.

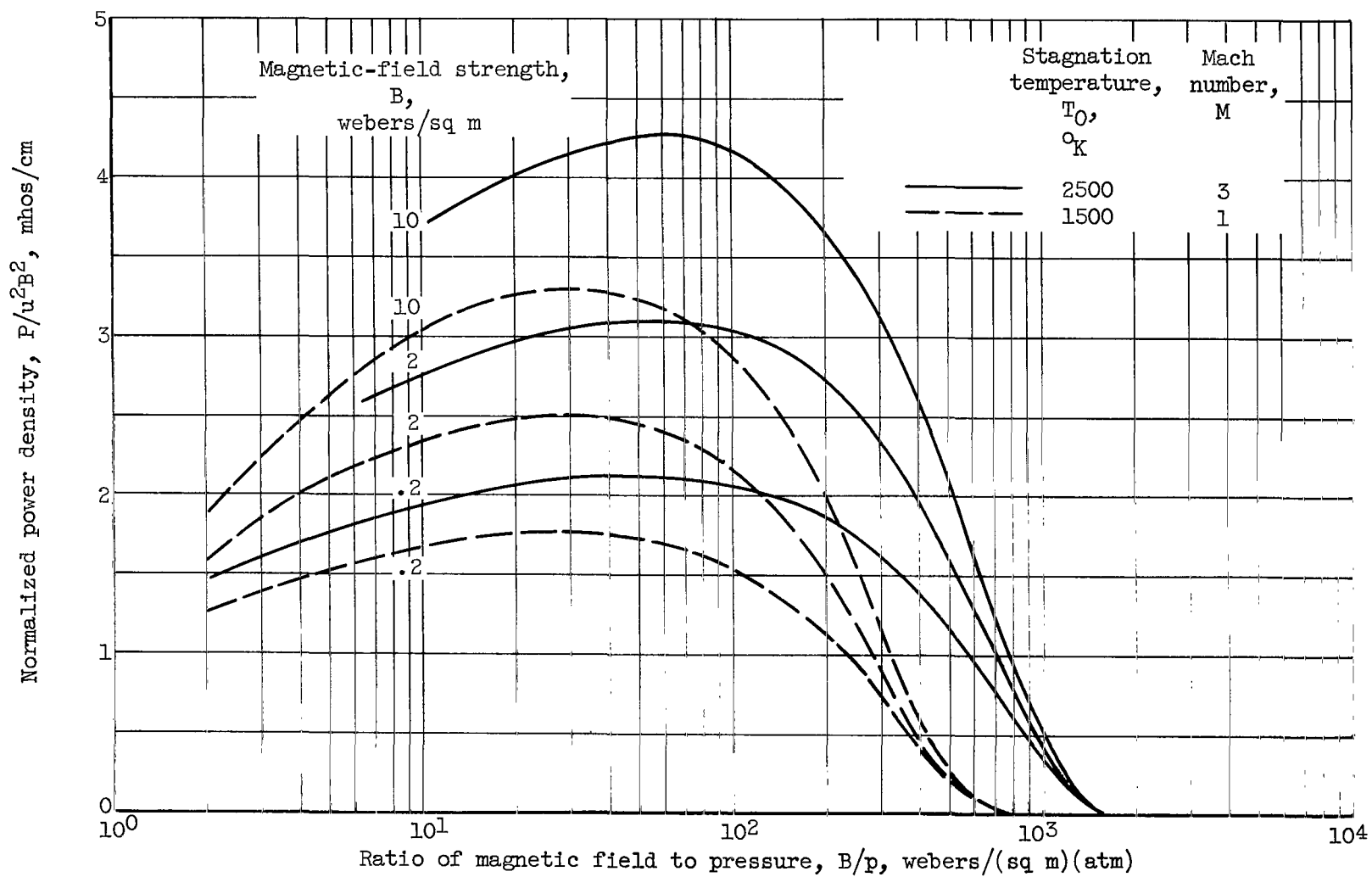


Figure 9. - Normalized power density as function of magnetic-field - pressure ratio.